

MICROCOPY RESOLUTION TEST CHART
NATIONAL BUREAU OF STANDARDS-1963-A

UNCLAS

SECURITY CLASSIFICATION OF THIS PAGE (When Data Entered)

2

REPORT DOCUMENTATION PAGE		READ INSTRUCTIONS BEFORE COMPLETING FORM
1. REPORT NUMBER	2. GOVT ACCESSION NO. AD-A133941	3. RECIPIENT'S CATALOG NUMBER
4. TITLE (and Subtitle) LOSS MECHANISMS IN LOW TEMPERATURE EXPANDERS		5. TYPE OF REPORT & PERIOD COVERED THESIS
		6. PERFORMING ORG. REPORT NUMBER
7. AUTHOR(s) SCHEIB, TIMOTHY E.		8. CONTRACT OR GRANT NUMBER(s)
9. PERFORMING ORGANIZATION NAME AND ADDRESS MASS. INST. OF TECHNOLOGY CAMBRIDGE, MA 02139		10. PROGRAM ELEMENT, PROJECT, TASK AREA & WORK UNIT NUMBERS
11. CONTROLLING OFFICE NAME AND ADDRESS CODE 031 NAVAL POSTGRADUATE SCHOOL MONTEREY, CA 93940		12. REPORT DATE JUN81
		13. NUMBER OF PAGES 76
14. MONITORING AGENCY NAME & ADDRESS (if different from Controlling Office)		15. SECURITY CLASS. (of this report) UNCLAS
		15a. DECLASSIFICATION/DOWNGRADING SCHEDULE
16. DISTRIBUTION STATEMENT (of this Report) APPROVED FOR PUBLIC RELEASE; DISTRIBUTION UNLIMITED		
17. DISTRIBUTION STATEMENT (of the abstract entered in Block 20, if different from Report)		
18. SUPPLEMENTARY NOTES		
19. KEY WORDS (Continue on reverse side if necessary and identify by block number) LOSS MECHANISMS LOW TEMPERATURE EXPANDERS		DTIC JUN 1983
20. ABSTRACT (Continue on reverse side if necessary and identify by block number) ATTACHED		

AD-A133941

DTIC FILE COPY

DD FORM 1473 JAN 73

EDITION OF 1 NOV 68 IS OBSOLETE
S/N 0102-014-6601

UNCLAS

SECURITY CLASSIFICATION OF THIS PAGE (When Data Entered)

ABSTRACT

used
An experimental study ~~was carried out to~~ investigated the actual influence of the boundary layer on heat transfer losses in typical expanders utilized in low temperature systems. More specifically, to investigate the effect of the boundary layer on the time dependence of the rate of heat transfer through the cylinder walls. The experimental expander utilized was a closed cylinder apparatus with a fixed mass charge of helium gas. Cyclic pressure and volume data points were generated during operation of the expander. The resulting experimental pressure vs. volume data trace was stored digitally and presented graphically using a Nicolet storage oscilloscope. The CMS computer system was used to further reduce and interpret the data. *It was*

The results concluded that the temperature of the boundary layer gas had the controlling effect over the cylinder bulk gas temperature in determining the actual rate of heat transfer through the cylinder walls. The apparent zero rate of heat transfer point occurred when the bulk gas temperature equaled the cylinder wall temperature. Because of the strong effect that the boundary layer had on the heat transfer in the cylinder, the actual zero rate of heat transfer point occurred when the boundary layer gas temperature equaled the cylinder wall temperature. The boundary layer gas temperature was determined responsible for up to a 64 degree phase difference in the times of the actual and apparent zero rate of heat transfer points in the compression and expansion strokes in the cylinder. This phase difference was evaluated to be leading in both cases. Therefore the actual time of zero rate of heat transfer preceded the apparent time of zero rate of heat transfer by a significant margin in each piston stroke. *A*

LOSS MECHANISMS IN LOW TEMPERATURE EXPANDERS

by

TIMOTHY EDWARD SCHEIB

B.S., United States Naval Academy
(1973)

SUBMITTED TO THE DEPARTMENT OF
OCEAN ENGINEERING IN PARTIAL
FULFILLMENT OF THE REQUIREMENTS
FOR THE DEGREES OF

OCEAN ENGINEER

and

MASTER OF SCIENCE

at the

MASSACHUSETTS INSTITUTE OF TECHNOLOGY

May 1981

© Timothy Edward Scheib 1981

The author hereby grants to M.I.T. permission to reproduce
and to distribute copies of this thesis document in whole
or in part.

Signature of Author

Timothy Edward Scheib

Department of Ocean Engineering
May 8, 1981

Certified by

Joseph L. Smith, Jr.

Joseph L. Smith, Jr.
Thesis Supervisor

Accepted by

A. Douglas Carmichael

A. Douglas Carmichael
Chairman, Departmental Graduate Committee



Accession For	
NTIS GRA&I	<input checked="" type="checkbox"/>
DTIC TAB	<input checked="" type="checkbox"/>
Unannounced	<input type="checkbox"/>
Justification	<input type="checkbox"/>
By _____	
Distribution/	
Availability Codes	
Avail and/or	
Dist	Special
A	

LOSS MECHANISMS IN LOW TEMPERATURE EXPANDERS

by

TIMOTHY EDWARD SCHEIB

Submitted to the Department of Ocean Engineering
on May 3, 1981 in partial fulfillment of the
requirements for the degree of Ocean Engineer and
the degree of Master of Science in
Mechanical Engineering

ABSTRACT

An experimental study was carried out to investigate the actual influence of the boundary layer on heat transfer losses in typical expanders utilized in low temperature systems. More specifically, to investigate the effect of the boundary layer on the time dependence of the rate of heat transfer through the cylinder walls. The experimental expander utilized was a closed cylinder apparatus with a fixed mass charge of helium gas. Cyclic pressure and volume data points were generated during operation of the expander. The resulting experimental pressure vs. volume data trace was stored digitally and presented graphically using a Nicolet storage oscilloscope. The CMS computer system was used to further reduce and interpret the data.

The results concluded that the temperature of the boundary layer gas had the controlling effect over the cylinder bulk gas temperature in determining the actual rate of heat transfer through the cylinder walls. The apparent zero rate of heat transfer point occurred when the bulk gas temperature equaled the cylinder wall temperature. Because of the strong effect that the boundary layer had on the heat transfer in the cylinder, the actual zero rate of heat transfer point occurred when the boundary layer gas temperature equaled the cylinder wall temperature. The boundary layer gas temperature was determined responsible for up to a 64 degree phase difference in the times of the actual and apparent zero rate of heat transfer points in the compression and expansion strokes in the cylinder. This phase difference was evaluated to be leading in both cases. Therefore the actual time of zero rate of heat transfer preceded the apparent time of zero rate of heat transfer by a significant margin in each piston stroke.

Thesis Supervisor: Dr. Joseph L. Smith, Jr.

Title: Professor of Mechanical Engineering

ACKNOWLEDGEMENTS

I thank my thesis advisor, Professor Joseph L. Smith, Jr., for his guidance and support which was essential for the development of this thesis. I also thank Henry Faulkner for his invaluable assistance. Finally, I thank my wife, Cheryl, and children, Holly and Skip, for their undying patience and understanding during these past three years. Without their help not a word of this thesis would have been possible.

TABLE OF CONTENTS

	<u>Page</u>
Title Page.	1
Abstract.	2
Acknowledgements.	3
Table of Contents	4
List of Figures	6
Definition of Symbols Used.	7
Chapter I - Introduction.	9
I.A. - Calculation of Loss.	11
I.B. - Boundary Layer Effects	14
I.C. - Phase Difference in Heat Flux.	16
Chapter II - Description of Test Equipment and Testing Procedure.	23
II.A. - Experimental Expander	23
II.B. - Pressure Measurement.	25
II.C. - Volume Measurement.	25
II.D. - Cylinder Wall Temperature Measurement .	26
II.E. - Digital Storage Oscilloscope.	26
II.F. - Testing Procedure	28
Chapter III - Computer Reduction and Interpretation of Data	30
III.A. - Computer Inputs.	30
III.B. - Calculation of Reference Points.	31
III.C. - System Mass Calculation.	32
III.D. - Calculation of Temperature and Entropy.	32
III.E. - Calculation of System Losses	33

III.F. - Non-Dimensional Parameter Calculations	34
F.1. Non-Dimensional Volume	34
F.2. Non-Dimensional Pressure	35
F.3. Non-Dimensional Temperature.	35
F.4. Non-Dimensional Entropy.	35
F.5. Non-Dimensional System Losses.	36
III.G. - Computer Output.	36
Chapter IV - Results.	38
Chapter V - Discussion.	42
V.A. - Data Point Scatter	42
V.B. - Shape of Temperature vs. Entropy Plots	44
V.C. - Identification of the Adiabatic Points in the Cycle	47
V.D. - Effects of the Boundary Layer.	48
V.E. - Explanation of the Phase Difference.	50
Chapter VI - Conclusions.	53
References.	55
Appendices.	56
A. - Cycle Fortran Program Listing.	56
B. - Cycle Data File Listing.	60
C. - Cycle Program Data Output.	65
D. - Cycle Program Plots Output	71

LIST OF FIGURES

	<u>Page</u>
1. Pressure vs. Volume Diagram for an Ideal Cycle of a Closed Cylinder Containing a Fixed Mass. . . .	13
2. Pressure vs. Volume Diagram for a Non-Ideal Cycle of a Closed Cylinder Containing a Fixed Mass. . . .	13
3. Schematic of Basic Heat Flow with Boundary Layer. . .	15
4. Pressure vs. Volume Diagram of System with Zero Boundary Layer Heat Capacitance	19
5. Pressure vs. Volume Diagram of System with Non-Zero Boundary Layer Heat Capacitance.	20
6. Temperature vs. Entropy Diagram for a Single Cycle	22
7. Diagram of Experimental Expander.	24
8. Schematic of Volume Indicator	27
9. TSTR vs. SSTR Smooth Curve Trace with Adiabatic and Isothermal Limits and Compression and Expansion Stroke Phase Differences.	39
10. Non-Dimensional Temperature vs. Non-Dimensional Entropy Plot Annotated with Minimum and Maximum Values.	45
11. Pressure vs. Volume Plot with Adiabatic Points Annotated	49

DEFINITION OF SYMBOLS USED

<u>Symbol</u>	<u>Definition</u>	<u>Units</u>
A	heat transfer area	in ²
C _p	specific heat at constant pressure	Btu/lb _m ^{-°R}
C _v	specific heat at constant volume	Btu/lb _m ^{-°R}
h	surface coefficient of heat transfer	Btu/hr-ft ² -°R
m	system mass	lb _m
P	cylinder pressure	lb _f /in ²
P _o	reference cylinder pressure	lb _f /in ²
P _{comp}	compression stroke pressure at reference volume	lb _f /in ²
P _{exp}	expansion stroke pressure at reference volume	lb _f /in ²
P _{mep}	mean pressure over the compression stroke (eqn 21)	lb _f /in ²
PSTR	non-dimensionalized pressure (eqn 22)	--
q	rate of heat transfer	in-lb _f /sec
Q	quantity of heat transferred	in-lb _f
R	specific gas constant	ft-lb _f /lb _m ^{-°R}
RPM	piston revolutions per minute	rev/min
S	entropy of cylinder bulk gas	in-lb _f /°R
SSTR	non-dimensionalized entropy (eqn 24)	--
t	time	sec

<u>Symbol</u>	<u>Definition</u>	<u>Units</u>
$T, T_{\text{bulk gas}}$	cylinder bulk gas temperature	$^{\circ}\text{R}$
T_0	reference temperature	$^{\circ}\text{R}$
$T_{\text{boundary layer}}$	boundary layer gas temperature	$^{\circ}\text{R}$
T_{wall}	cylinder wall temperature	$^{\circ}\text{R}$
TSTR	non-dimensionalized temperature (eqn 23)	--
U	internal energy	in-lb _f
V	cylinder volume	in ³
V_0	reference cylinder volume	in ³
VBDC	cylinder volume at piston bottom dead center position	in ³
VTDC	cylinder volume at piston top dead center position	in ³
VSTR	non-dimensionalized cylinder volume (eqn 20)	--
W	total cylinder work	in-lb _f
W_{comp}	work done during compression stroke	in-lb _f
W_{exp}	work done during expansion stroke	in-lb _f
	ratio of specific heats (C_p/C_v)	--

CHAPTER I
INTRODUCTION

The reciprocating piston-cylinder system is a common and relatively simple device used in many different applications in today's mechanical world. Each day some type of reciprocating piston-cylinder system impacts on our lives whether it be through a reciprocating automotive engine or through some other type of reciprocating pumping device that may provide another personal service. An additional example of this type of device is a reciprocating cryogenic expander, whose purpose is to produce a reduction in the temperature of the gas passing through it.

In all of these types of systems work is produced through the expansion of a fluid against a piston. For an ideal expansion engine the expansion stage should be isentropic and the work per unit mass should be expressed as:

$$W = C_p (T_1 - T_2) \quad (1)$$

However, because this fluid expansion is not an ideal process, losses and inefficiencies are evident. Some examples of typical loss mechanisms usually associated with through flow expanders are:

1. clearance losses - Because of the clearance volume remaining when the piston is at top dead center, the cylinder cannot fully exhaust the entire old charge. There-

fore the fresh charge entering the piston is further limited in the actual volume that it can ideally occupy. The clearance losses then define these variations from the ideal case. The actual factors responsible for the clearance loss include much more complex processes such as blow in-blow out loss effects and the intricate influences of the mass flow rate. These processes are extremely involved and their evaluation here is not required, so then just calling attention to their existence will suffice.

2. valve losses - Because the inlet and exhaust valves are responsible for a resistance to the fluid flow, there will be a pressure drop across the valves that will account for some loss.

3. piston ring losses - There will be some loss associated with the leakage past the piston rings. Also any friction between the piston rings and cylinder walls will generate some heat that will be transferred to the fluid and add to the loss.

The above examples are certainly not the only loss mechanisms evident in a piston-cylinder arrangement, but they are usually considered the prominent factors.

This experimental investigation will consider the loss mechanisms evident in a closed cylinder. No inlet or exhaust processes will be evaluated. The mass of the working fluid will remain constant throughout the compression expansion cycle being examined. Therefore the causes of the

losses evident in the cylinder will simplify, as the heat transfer loss will be the only prominent loss mechanism. This will then permit the determination of the actual effect that the heat transfer loss has on the system.

I.A. Calculation of Loss

To evaluate the thermodynamic processes occurring in the closed piston-cylinder the first law of thermodynamics will be utilized. In its most basic form the first law states that

$$dQ = dU + dW. \quad (2)$$

If the pressure of the gas is spatially uniform at each state of the cycle and the work done by the gas is restricted to the displacement of the piston, then the work term can be defined as

$$dW = \int PdV. \quad (3)$$

For an ideal gas the change in internal energy of the gas is

$$dU = mC_v dT_{\text{bulk gas}}. \quad (4)$$

The first law can then be expressed as

$$\int PdV = dQ - mC_v dT_{\text{bulk gas}}. \quad (5)$$

If the process is assumed to be ideal and adiabatic, then the heat transfer in the system will be zero ($dQ = 0$)

and the first law will then simplify to

$$\int PdV = mC_v dT_{\text{bulk gas.}} \quad (6)$$

When dT is eliminated by substitution of the ideal gas equation of state, equation (5) integrates to

$$PV^\gamma = \text{constant.} \quad (7)$$

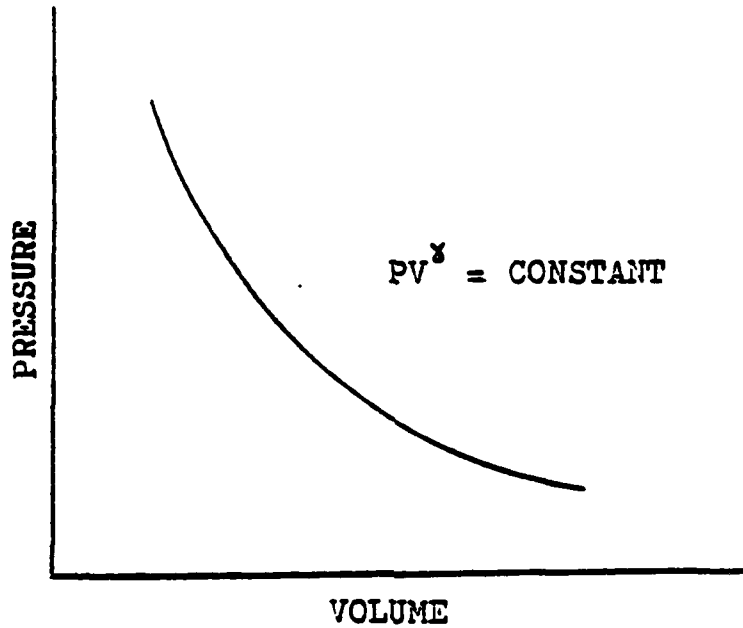
The construction of the trace for this process on a pressure vs. volume diagram will yield a plot in which the compression and expansion processes share the same line and therefore describe no enclosed area (Figure 1). There will be zero net work done on the working fluid.

If the process is not ideal, the compression-expansion trace will not follow the $PV^\gamma = \text{constant}$ path. Plotting the non-ideal expansion trace on a pressure vs. volume diagram will yield a closed plot circumscribing some enclosed area (Figure 2). This enclosed area represents the net work done on the working fluid during the cycle and also represents the total losses that the system experiences during the cycle.

Therefore the total loss per cycle in the piston-cylinder arrangement can be expressed as the integral of pressure times a differential volume around the entire cycle

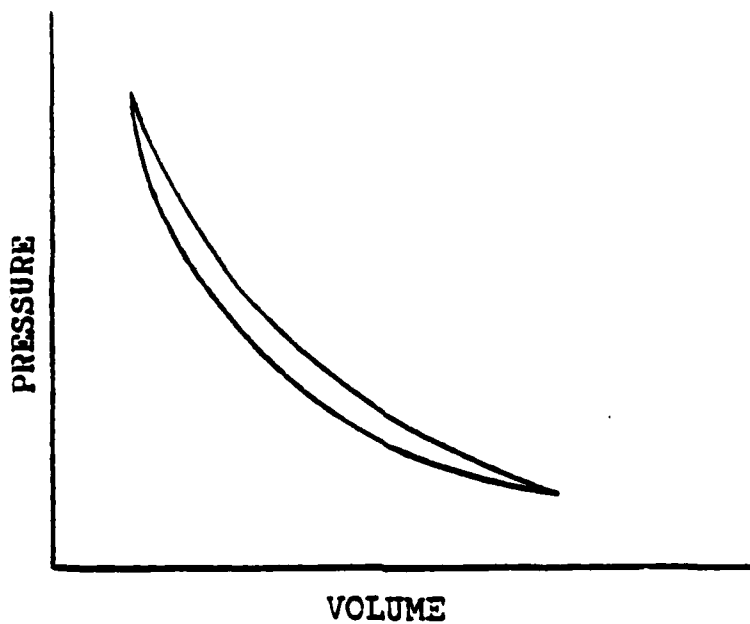
$$\oint PdV = \text{loss.} \quad (8)$$

This loss is specifically associated with just the bulk gas



PRESSURE VS. VOLUME DIAGRAM FOR AN IDEAL CYCLE OF
A CLOSED CYLINDER CONTAINING A FIXED MASS

FIGURE 1



PRESSURE VS. VOLUME DIAGRAM FOR A NON-IDEAL CYCLE
OF A CLOSED CYLINDER CONTAINING A FIXED MASS

FIGURE 2

in the cylinder. The total loss per cycle can also be expressed in a different form by considering the loss as the integral of the rate of heat transfer from the bulk gas through the wall around the entire cycle

$$\oint q \, dt = \text{loss.} \quad (9)$$

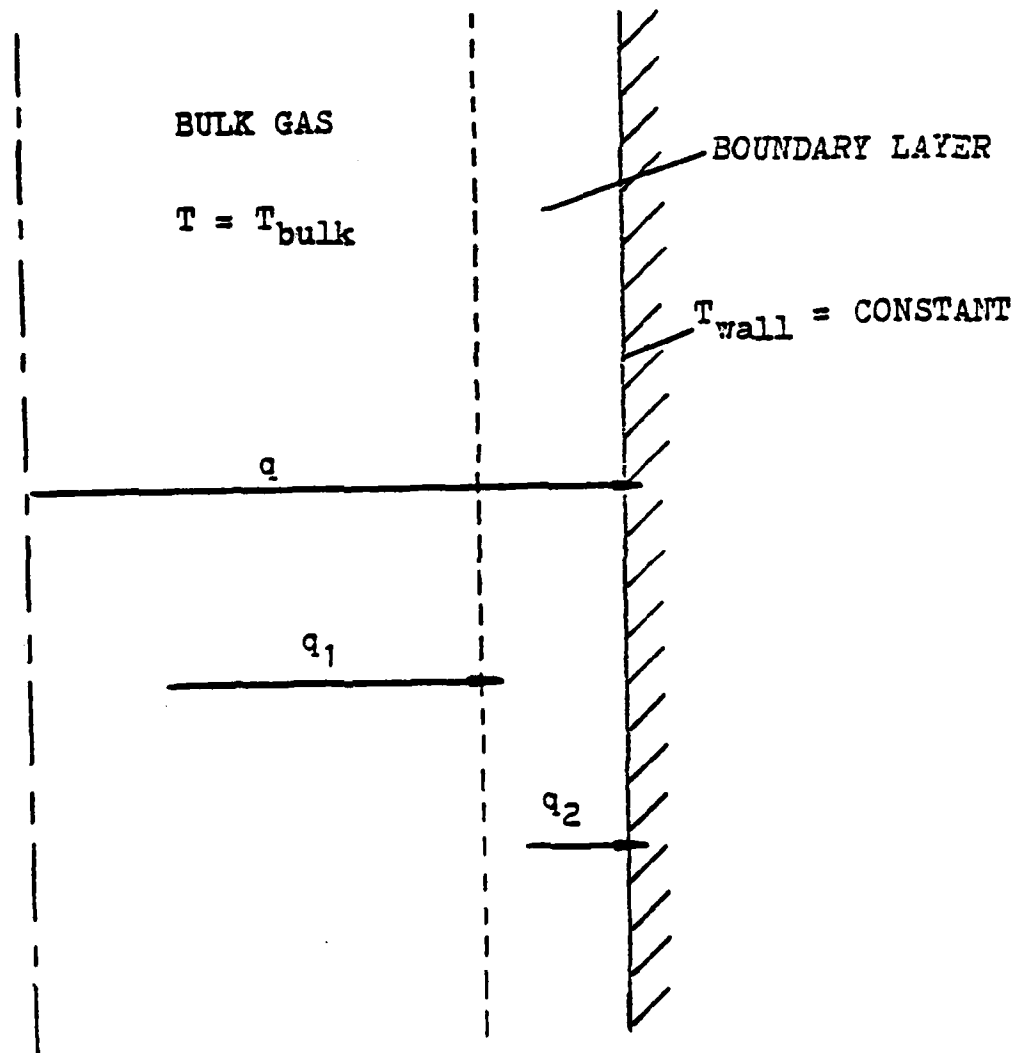
I.B. Boundary Layer Effects

Adjacent to the inside of the cylinder wall a small volume of gas with finite mass will permanently exist through which the heat flux must travel in order to reach the cylinder wall. As the piston moves in the cylinder, the depth of this thin layer of gas will vary constantly due to well defined boundary layer effects. If the cyclic heat flow entering and exiting the boundary layer is considered, the importance of the boundary layer effect can be illustrated (Figure 3).

For an entire cycle the total loss from the bulk gas to the wall ($\oint q \, dt$) should be equal to the loss from the bulk gas to the boundary layer ($\oint q_1 \, dt$) and should also be equivalent to the loss from the boundary layer to the wall ($\oint q_2 \, dt$).

$$\oint q \, dt = \oint q_1 \, dt = \oint q_2 \, dt \quad (10)$$

Because the heat capacitance of the cylinder wall is very great when compared to the heat capacitance of the gas, the wall temperature can be assumed to be constant when



SCHEMATIC OF BASIC HEAT FLOW WITH BOUNDARY LAYER

FIGURE 3

considering a single cycle.

If the small volume of gas comprising the boundary layer had no heat capacitance then at any instant during the cycle the rate of heat transfer from the bulk gas to the boundary layer would equal the rate of heat transfer from the boundary layer to the cylinder wall.

$$q = q_1 = q_2 \quad \left(\begin{array}{l} \text{instantaneous, zero heat} \\ \text{capacitance in boundary layer} \end{array} \right) \quad (11)$$

However, the presence of this boundary layer would suggest that it would hold some finite value of heat capacitance between the temperature extremes of the bulk gas and the cylinder wall. Assuming that the boundary layer does support some heat capacitance, then as the piston moves through the cylinder the actual rate of heat transfer from the bulk gas to the boundary layer should instantaneously differ from the rate of heat transfer from the boundary layer to the cylinder wall.

$$q \neq q_1 \neq q_2 \quad \left(\begin{array}{l} \text{instantaneous, finite heat} \\ \text{capacitance in boundary layer} \end{array} \right) \quad (12)$$

I.C. Phase Difference in Heat Flux

The rate of heat transfer and therefore the loss experienced from the system depends heavily upon the temperature difference between the working gas and the cylinder wall and upon the properties of the working gas.

$$q = hA (T_{\text{gas}} - T_{\text{wall}}) \quad (13)$$

During both the compression and the expansion stroke of a cycle, the system will pass through a point where the gas temperature will equal the cylinder wall temperature. At these two points the rate of heat transfer will equal zero as the temperature difference will equal zero ($T_{\text{gas}} - T_{\text{wall}} = 0$). Consider a system in which the cylinder wall boundary layer has zero heat capacitance. Here the temperature of the gas in the layer adjacent to the wall will be approximately equal to the bulk gas temperature. Therefore at the points in the cycle where the bulk gas temperature equals the cylinder wall temperature, the process will be adiabatic and the rate of heat transfer will equal zero.

However, if the system is assumed to have finite heat capacitance in the thermal boundary layer, the temperature of the gas in the layer adjacent to the wall could differ significantly from the bulk gas temperature. In this system the points of zero rate of heat transfer will not occur where $T_{\text{bulk gas}} = T_{\text{wall}}$, but will occur at the points where $T_{\text{boundary layer}} = T_{\text{wall}}$.

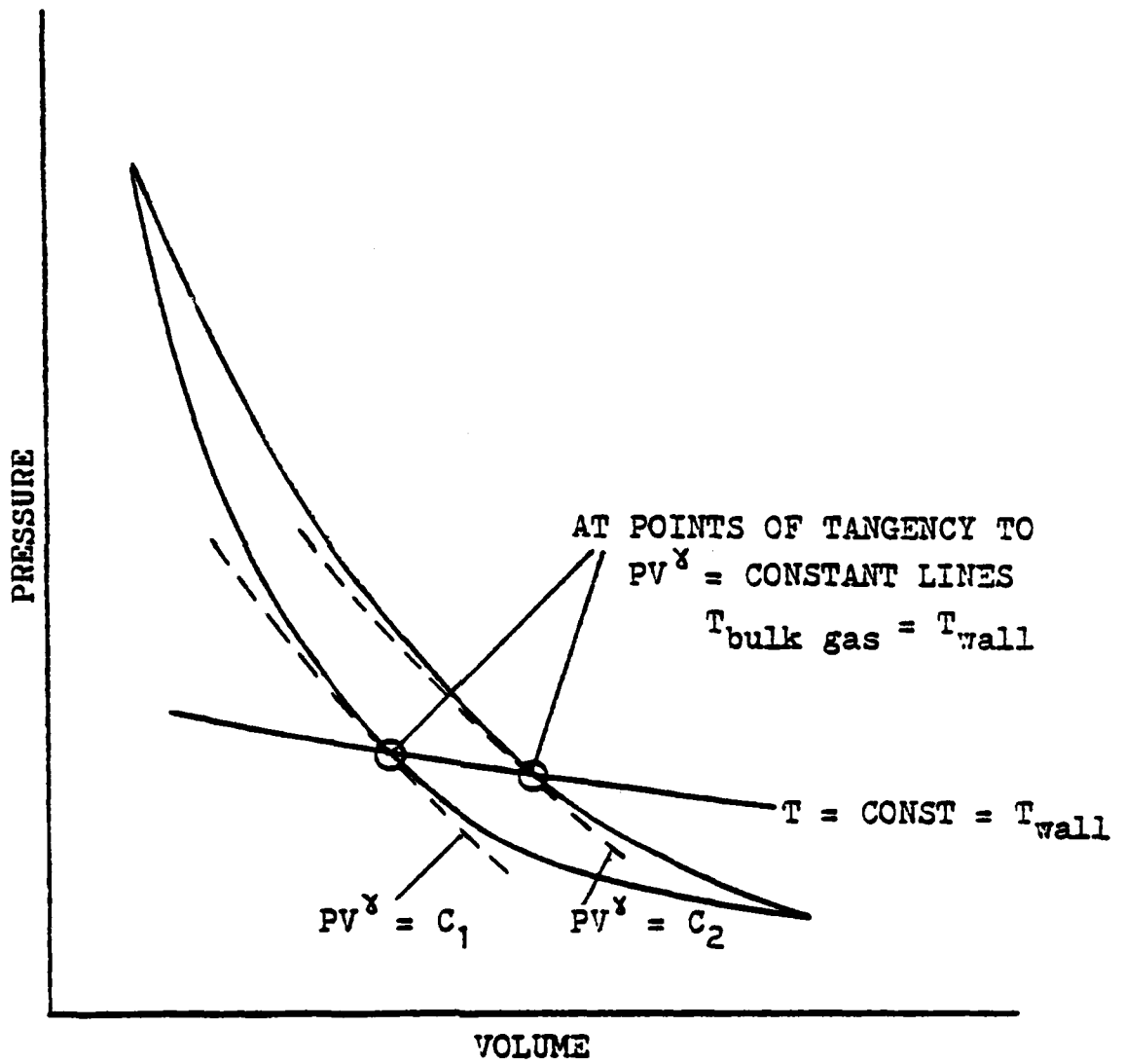
To illustrate this difference, if the compression expansion process is plotted on a pressure vs. volume diagram, the points of zero rate of heat transfer will occur where the process is adiabatic at that point. Previously in this section it was shown that the process will be adiabatic at the point where the trace is tangent to a line where $PV^\gamma = \text{constant}$. Figure 4 illustrates a pressure vs. volume

diagram for a system where the points of tangency to the adiabatic lines coincide with the points where the bulk gas temperature equals the cylinder wall temperature.

If a system with finite heat capacitance in the boundary layer is considered, the points at which the bulk gas temperature equal the cylinder wall temperature will not coincide with the points at which the system trace is tangent to the adiabatic lines. Figure 5 illustrates this difference. In both the compression and expansion stroke, a phase difference is identified that is the difference (in time or degrees of rotation) between the points of actual zero rate of heat transfer in the system (points where the process is perfectly adiabatic where $T_{\text{boundary layer}} = T_{\text{wall}}$) and the points of apparent zero rate of heat transfer in the system (points where $T_{\text{bulk gas}} = T_{\text{wall}}$).

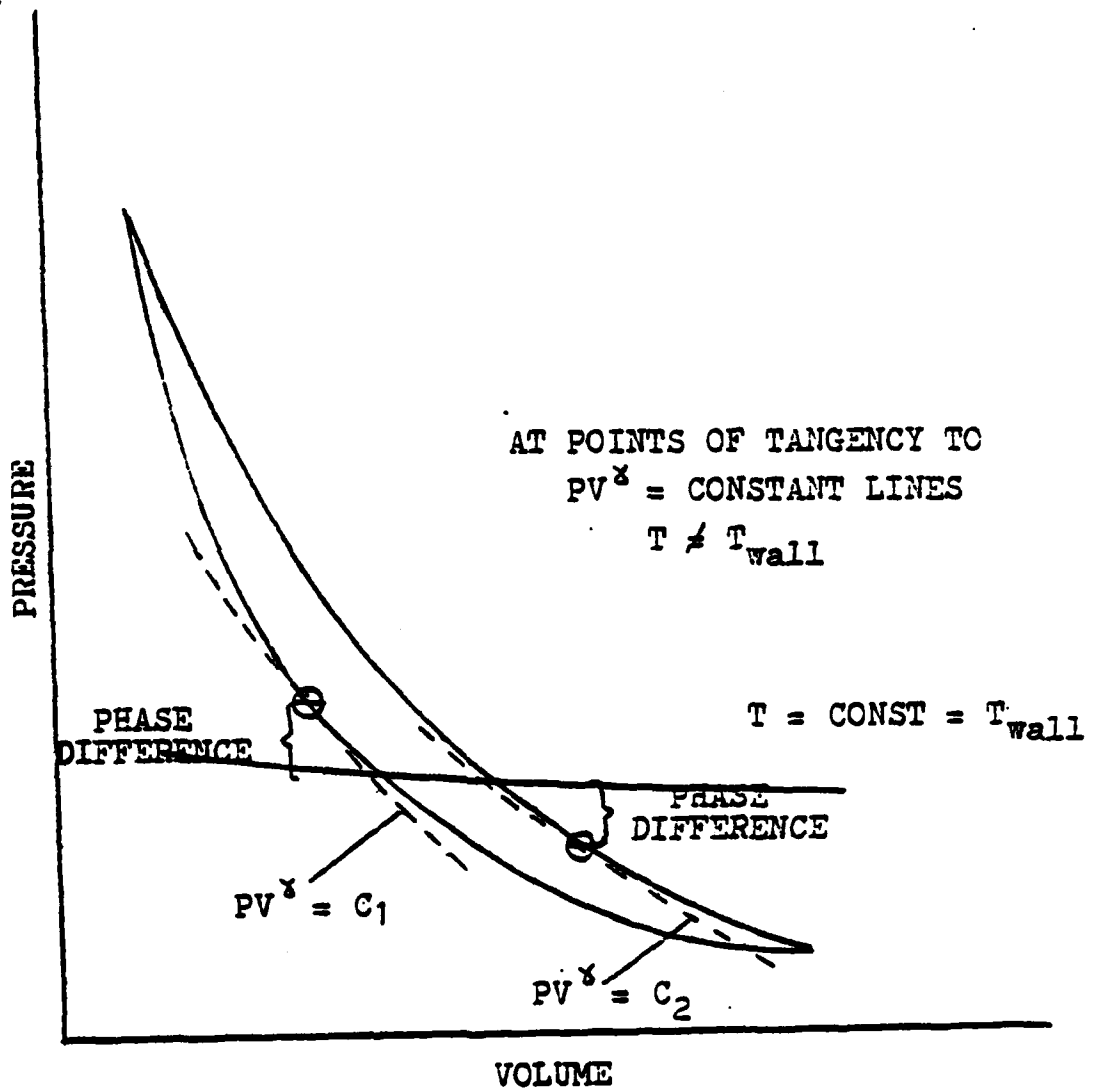
Therefore the effect of the boundary layer on the heat transfer in the cylinder must be determined in order to evaluate the impact of the boundary layer on the total system loss.

Other methods are certainly available that would facilitate calculation of the net cyclic loss and any phase difference experienced in the points of zero rate of heat transfer. One of the most direct and accurate methods requires the plotting of a temperature vs. entropy diagram for the cycle. Figure 6 is an example of such a trace. The area enclosed by the curve represents the net work done on



PRESSURE VS. VOLUME DIAGRAM OF SYSTEM
WITH ZERO BOUNDARY LAYER HEAT CAPACITANCE

FIGURE 4



PRESSURE VS. VOLUME DIAGRAM OF A SYSTEM WITH
 NON-ZERO BOUNDARY LAYER HEAT CAPACITANCE

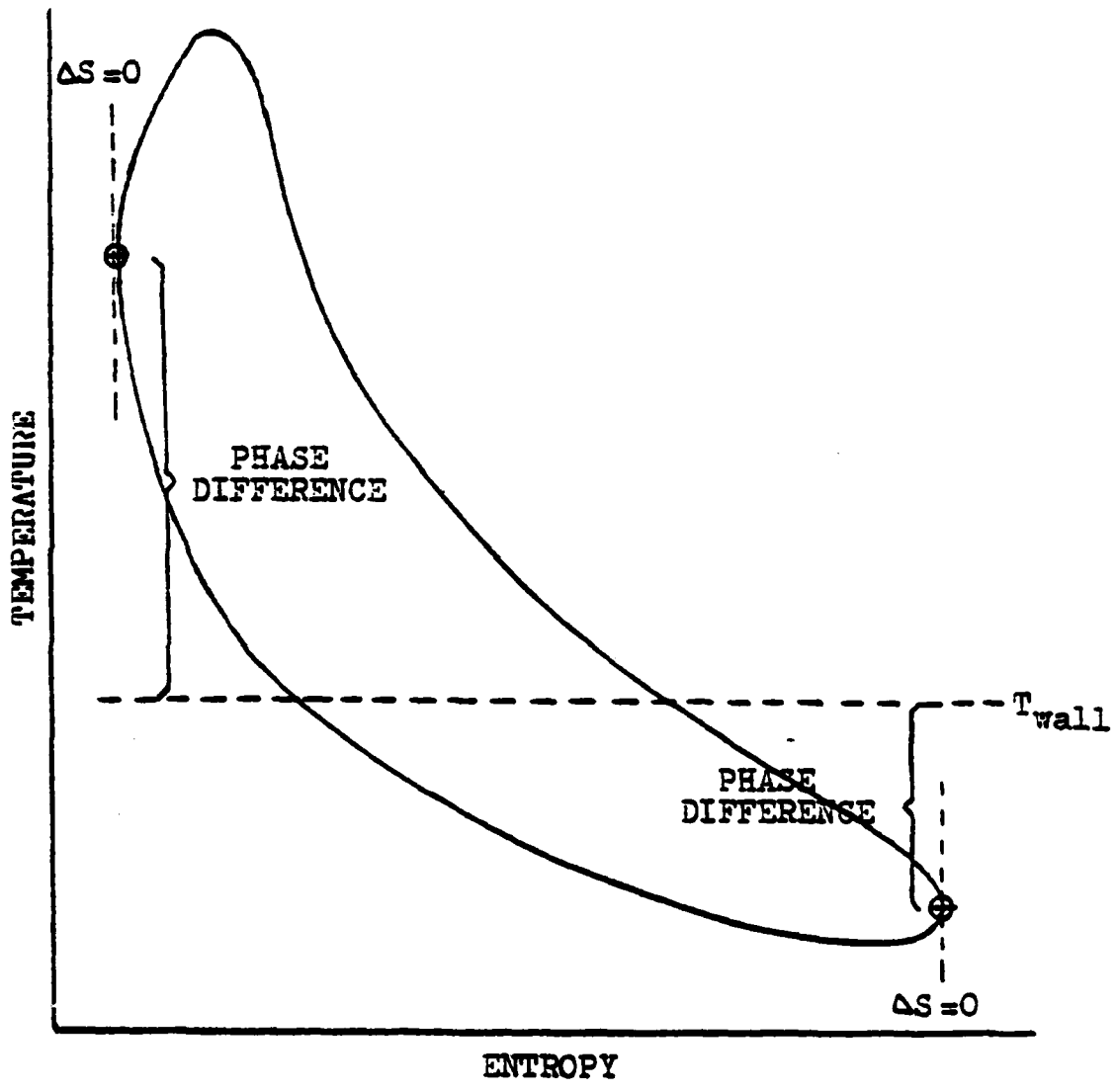
FIGURE 5

the working fluid which is also equivalent to the total loss experienced during the cycle. For any single cycle the following statement should be true:

$$\oint PdV = \oint TdS = \text{loss.} \quad (14)$$

On this temperature vs. entropy diagram, the points on the trace that are tangent to a vertical line signify points where the change in entropy is equal to zero. At these points the process is perfectly adiabatic and signify points of zero rate of heat transfer. The temperature of the gas adjacent to the cylinder wall at these points should be equal to the temperature of the cylinder walls. If these points of actual zero rate of heat transfer differ from the points on the graph of apparent zero rate of heat transfer (where $T_{\text{bulk gas}} = T_{\text{wall}}$), then some phase difference exists. In Figure 6 a phase difference is evident in both the compression and expansion strokes.

The existence of this phase difference must be proven and then evaluated in order to provide information necessary to quantify the impact of the thermal boundary layer effects on the total system loss.



TEMPERATURE VS. ENTROPY DIAGRAM FOR A SINGLE CYCLE

FIGURE 6

CHAPTER II

DESCRIPTION OF TEST EQUIPMENT AND TESTING PROCEDURE

II.A. Experimental Expander

The apparatus used to investigate the theoretical processes of the expander was composed primarily of the motor and cylinder body of a modified air compressor. The active cylinder was bolted directly on top of the original compressor cylinder. This cylinder included the gas charging port, temperature and pressure measuring instruments and had the additional capability of water cooling the cylinder. A diagram of this apparatus is shown in Figure 7. The piston utilized to compress and expand the gas was housed in the active cylinder. The active cylinder bore was 2.00 inches and the piston stroke was 3.00 inches. During operation the piston remained within the cylinder, while its maximum upward travel at the top dead center position moved the piston to the upper lip of the cylinder.

The cylinder extension housed a stationary piston that formed the head of the cylinder volume. A threaded bolt extending through the top of the extension cylinder and into the stationary piston provided the additional capability of changing the volume ratio. By raising or lowering the stationary piston through its four inch range with this threaded bolt, the cylinder provided volume ratios ranging from 1.5 to 2.4.

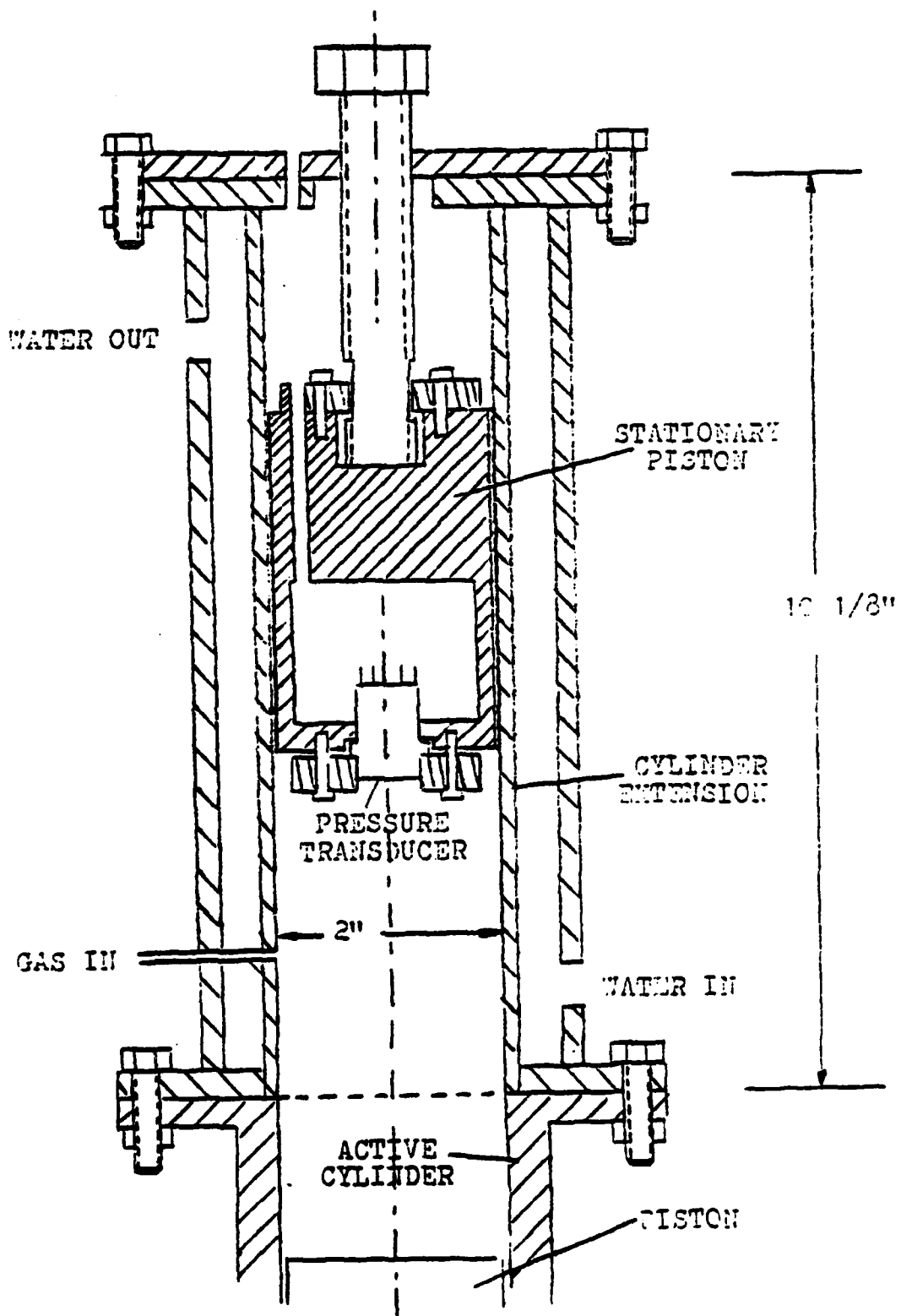


DIAGRAM OF EXPERIMENTAL EXPANDER

FIGURE 7

II.B. Pressure Measurement

A strain gage pressure transducer was utilized to measure cylinder pressure. The pressure measurement is determined in this type of transducer by the fact that the resistance of the transducer strain gages on the pressure sensitive surface changes in proportion to the pressure on the surface. The transducer output is then proportional to the cylinder pressure. The transducer mounted in the cylinder head was of the range 0 to 100 psi and was calibrated at 4.342 psi/millivolt for a 6.0 volt input. In order to calculate the cylinder pressure, the transducer output at a known pressure had to be determined. Therefore prior to recording any experimental data, the transducer input at atmospheric pressure was recorded to provide the required pressure reference. To make this step easier a balance box was installed with the pressure transducer which permitted the setting of a known pressure directly on the oscilloscope.

II.C. Volume Measurement

The method utilized to measure the cylinder volume consisted of a circular cam mounted eccentrically on the compressor crankshaft. Because each cycle of the compressor piston corresponded to one revolution of the compressor crankshaft, the angle of a given spot on the circumference of the shaft was directly proportional to the position of the compressor piston and therefore was also proportional to

the cylinder volume. A follower was mounted on the outer diameter of the circular cam so that the displacement of the follower was proportional to the displacement of the piston. This system is displayed in Figure 8.

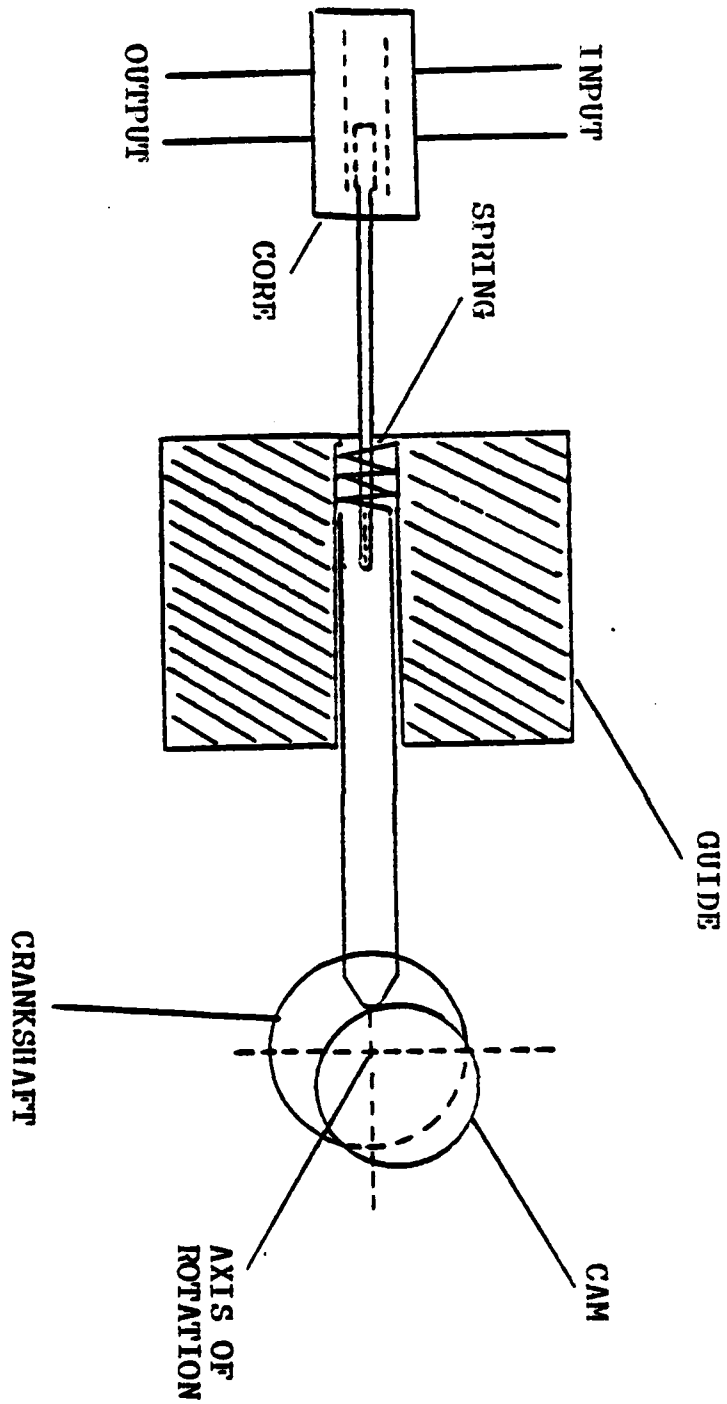
An HP 7DCT displacement transducer was connected to the follower and provided a D.C. output that was proportional to the displacement of the follower. The calibration of the transducer provided the maximum output signal when the cylinder volume was maximum at the piston bottom dead center position. By knowing the maximum and minimum cylinder volume for the experimental run, the intermediate values for cylinder volume could easily be calculated by using the transducer output.

II.D. Cylinder Wall Temperature Measurement

Four thermocouples were utilized to measure the average cylinder wall temperature during testing. Three thermocouples monitored the temperature at different locations on the outside of the cylinder wall. The remaining thermocouple was placed on the outside of the cylinder cooling water jacket. The output of the thermocouples was displayed using an Autodata Nine Digital data logger that provided a continuous readout in degrees Centigrade.

II.E. Digital Storage Oscilloscope

The output of the pressure and volume transducers was provided as input to a Nicolet Digital Oscilloscope Model



SCHMATIC OF VOLUME INDICATOR

FIGURE 8

206. The signal information provided to the scope was converted to digital form, stored in a buffer memory and then was displayed graphically. Digital information for each point remained available in storage. The Nicolet scope has the capability of storing up to 4096 data points. Because both pressure and volume were being monitored, each storage cycle consisted of 2048 pressure points and 2048 volume points. The scope had the capability of graphic display of either the pressure or volume trace vs. time or an X-Y axis plot of pressure vs. volume. The time interval between data points could be chosen on the scope to ensure that an entire cycle of data would be available in a single storage cell.

II.F. Testing Procedure

The following steps were performed in this order during the data acquisition run:

1. The position of the stationary piston was set properly.
2. The piston was moved to bottom dead center position and then checked by assuring that the output of the volume transducer was at a maximum.
3. The cylinder was opened to the atmosphere and the pressure transducer output was set on the oscilloscope and recorded.
4. The cylinder was charged with gas and the pressure transducer output recorded. At this point must ensure that the cylinder is not charged to a pressure that will over-pressurize the pressure transducer during compression.
5. The compressor motor was turned on and the oscilloscope set to automatically monitor a single cycle of the cylinder.

6. The cylinder wall temperatures were recorded immediately upon completion of the sample cycle.
7. The compressor motor was secured.
8. The pressure vs. volume data was monitored on the oscilloscope to ensure that the trace was satisfactory.

CHAPTER III

COMPUTER REDUCTION AND INTERPRETATION OF DATA

In order to efficiently interpret and display the raw data extracted from the Nicolet oscilloscope, the Institute's CMS computer system was used. The data was entered into the computer files and then was operated on to provide various thermodynamic parameters at each point. Using this information thermodynamic traces for the cycle were plotted. Finally the losses for the cycle were calculated by numerical integration of the curves.

III.A. Computer Inputs

The digital pressure vs. volume data provided by the Nicolet oscilloscope was input into a data file that was accessible to the main program. Other initial inputs required included:

1. The type of working gas used.
2. The specific gas constant for the gas (R).
3. The specific heat at constant pressure for the gas (C_p).
4. The specific heat at constant volume for the gas (C_v).
5. The cylinder volume at the top dead center position (VTDC).
6. The cylinder volume at the bottom dead center position (VBDC).
7. The total number of data points (P, V pairs) entered into the computer data file.
8. The time interval between data points.

9. The piston revolutions per minute.
10. The temperature readings from the cylinder wall thermocouples in degrees Centigrade.

III.3. Calculation of Reference Points

In order to have the capability of accurately comparing data at varying volume ratios, compressor speeds, and for different gases, computations performed on the data were done using common reference points. Therefore a standard method was required to determine each of the required temperature, volume and pressure reference points.

Cylinder bulk gas temperature was the first reference point determined and was set at 100°F. This temperature was chosen as it was a typical average cyclic temperature experienced in previous experimentation done with the same experimental cylinder apparatus. When expressed on the absolute scale the reference temperature was then set at the following value:

$$T_0 = 559.67^\circ \text{ R}$$

The method used to determine the reference volume consisted of calculating the geometric mean using the volume of the cylinder at the top dead center and bottom dead center positions. The actual formula for the determination of reference volume was

$$V_0 = \left(\frac{V_{BDC}}{V_{TDC}} \right)^{\frac{1}{2}} V_{TDC}. \quad (15)$$

Because the cylinder volume was expressed in units of cubic inches, the reference volume was also in cubic inches.

The determination of the reference pressure point required the prior determination of the reference volume point. Using the reference volume point, the pressures corresponding to this volume for both the compression and expansion strokes were found. The reference pressure was then determined to be the average of the compression and expansion pressure values at the reference volume.

$$P_o = \frac{P_{\text{comp}} + P_{\text{exp}}}{2} \quad (16)$$

Reference pressure was expressed in units of pounds force per square inch.

III.C. System Mass Calculation

In order to calculate the bulk gas temperature and entropy at each data point the system mass had to be determined. This calculation was performed using the ideal gas equation of state and the reference temperature, volume, and pressure values.

$$m = \frac{P_o V_o}{RT_o} \quad (17)$$

The system mass was then expressed in units of pounds mass.

III.D. Calculation of Temperature and Entropy

The bulk gas temperature at each data point was then

determined utilizing the ideal gas equation of state and other previously determined parameters.

$$T_i = \frac{P_i V_i}{R m} \quad (18)$$

The temperature values were expressed on the absolute scale in degrees Rankine.

The entropy value for each data point was calculated referenced to the previously determined values of reference volume and pressure by the relation

$$S_i - S_o = \Delta S = mC_v \ln \left[\frac{P_i}{P_o} \right] + mC_p \ln \left[\frac{V_i}{V_o} \right]. \quad (19)$$

The entropy values were expressed in units of inch-pounds force per degree Rankine.

III.E. Calculation of System Losses

In order to calculate the system losses during the cycle, cyclic traces of pressure vs. volume and temperature vs. entropy were plotted. The area enclosed within either of these closed curves should equal the total system loss.

$$\oint P dV = \oint T dS = \text{loss} \quad (14)$$

The integration was performed numerically using the trapezoid rule at each successive data point. Total area under the expansion curve was considered negative. The total system loss was then described in the units of negative

inch-pounds force.

An attempt was made to calculate the area using a much more involved and typically more accurate five point Gaussian quadrature integration method. However, because of the scatter of the digital data points near the ends of the curves, this method proved no more accurate than the much simpler trapezoid integration method.

III.F. Non-Dimensional Parameter Calculations

In order to provide the additional capability of comparing the computer output to the output data of any other similar apparatus, notwithstanding differences in the units involved, non-dimensional parameters were introduced. The computer routine then also included the calculations required to produce the output of non-dimensional values of pressure, volume, temperature and entropy. Plots were also made of non-dimensional pressure vs. volume and non-dimensional temperature vs. entropy in order to determine the non-dimensional loss values.

III.F.1. Non-Dimensional Volume

The volume data points were non-dimensionalized by dividing each data point by the total displaced volume of the cylinder.

$$VSTR_1 = \frac{V_1}{(VEBC-VTDC)} \quad (20)$$

III.F.2. Non-Dimensional Pressure

The cylinder pressure data points were non-dimensionalized by dividing each data point by a mean pressure calculated from the compression stroke. This mean pressure was defined as the total work added during the compression stroke divided by the total displaced volume of the cylinder.

$$P_{mep} = \frac{W_{comp}}{(VBDC-VTDC)} \quad (21)$$

Each pressure data point was then divided by this mean pressure during compression to find the non-dimensional pressure values.

$$PSTR_i = \frac{P_i}{P_{mep}} \quad (22)$$

III.F.3. Non-Dimensional Temperature

The bulk gas temperature data points were non-dimensionalized by dividing each data point by the reference temperature.

$$TSTR_i = \frac{T_i}{T_0} \quad (23)$$

III.F.4. Non-Dimensional Entropy

The entropy values were non-dimensionalized by dividing the calculated entropy values by the mean pressure during compression and the displaced volume of the cylinder and

then multiplying by the reference temperature.

$$SSTR = \frac{S_i T_o}{P_{mep} (VBDC-VTDC)} \quad (24)$$

III.F.5. Non-Dimensional System Losses

Non-dimensional values of total system loss were calculated in the same manner as the dimensional loss values were determined. Plots were made of non-dimensional pressure vs. volume and non-dimensional temperature vs. entropy and the enclosed areas were calculated by numerical integration utilizing the trapezoid method.

III.G. Computer Output

A listing of the Fortran computer program is displayed in Appendix A. A listing of the test data file used in the computations is presented in Appendix B.

The output of the computer routine includes the following data:

1. Pressure, volume, bulk gas temperature and entropy at each data point.
2. Non-dimensional pressure, volume, bulk gas temperature and entropy at each data point.
3. Piston revolutions per minute.
4. Time interval between data points.
5. Reference temperature volume and pressure values.
6. Average cylinder wall temperature.
7. System mass.

8. Pressure vs. volume plot.
9. Temperature vs. volume plot.
10. Temperature vs. entropy plot.
11. Non-dimensional pressure vs. non-dimensional volume plot.
12. Non-dimensional temperature vs. non-dimensional volume plot.
13. Non-dimensional temperature vs. non-dimensional entropy plot.
14. Calculations of dimensional and non-dimensional system loss.

An example of the computer output is displayed in Appendices C and D.

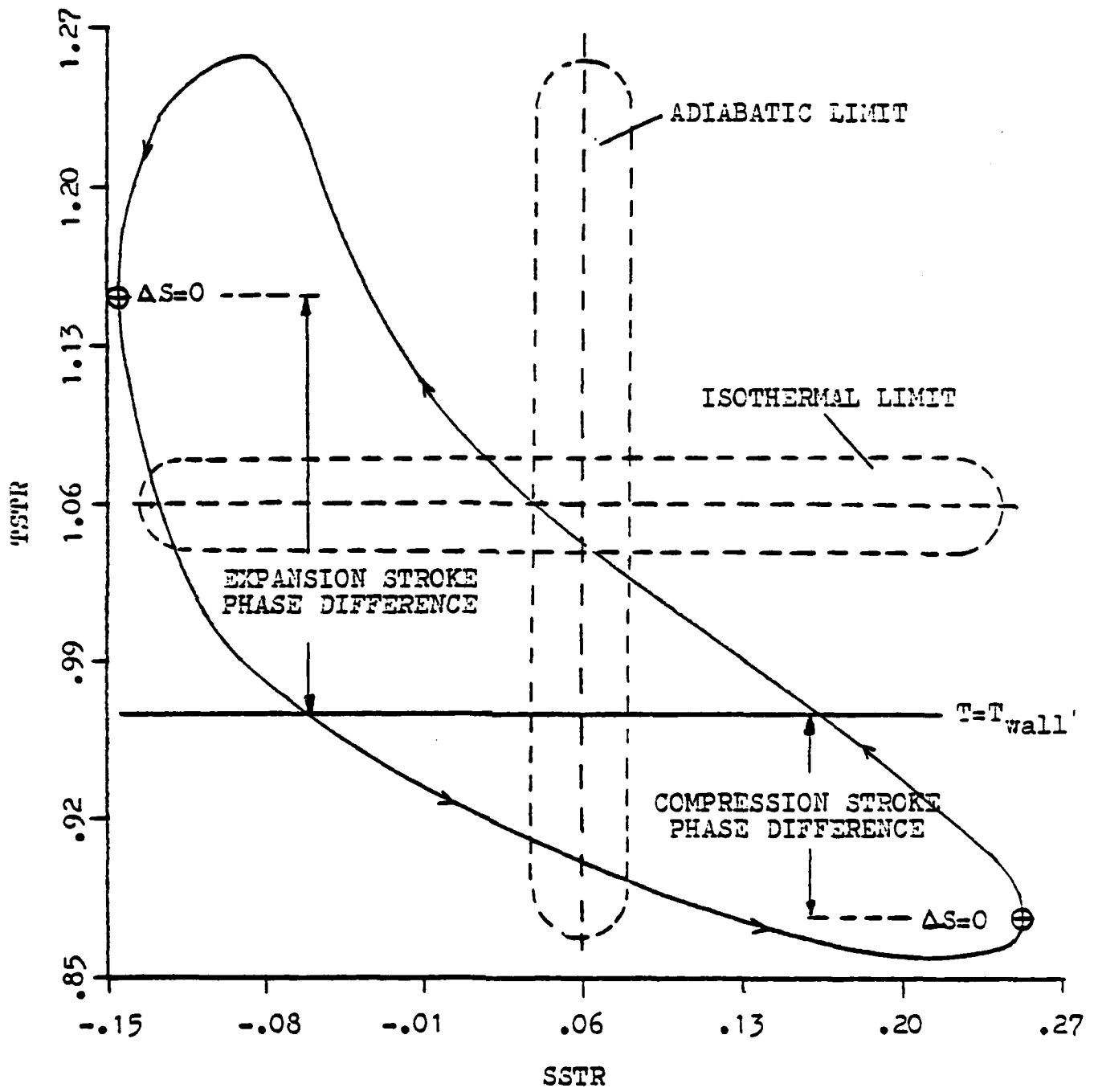
CHAPTER IV

RESULTS

The results of the single data set used are presented in the computer output in Appendices C and D. Helium was utilized in the cylinder as the working gas for the experiment.

The final pressure vs. volume and non-dimensional pressure vs. non-dimensional volume plots resulted in extremely smooth traces. Each depicted what could easily be identified as a conventional pressure vs. volume trace for this type of apparatus. Basically the same comment could be made about both the temperature vs. volume and non-dimensional temperature vs. non-dimensional volume plots. However, a greater degree of scatter seemed to be evident in the temperature vs. volume plots than in the pressure vs. volume plots.

In the temperature vs. entropy and non-dimensional temperature vs. non-dimensional entropy plots the scatter is much more evident. The shape of the trace also is somewhat different from a shape that one might expect the plot to have after first seeing the pressure vs. volume and temperature vs. volume traces. Figure 9 is a single line curve approximation of the TSTR vs. SSTR computer trace from Appendix D. The figure shows the adiabatic and isothermal limits of a plot of this type. The adiabatic limit being a curve where the compression and expansion strokes



TSTR VS. SSTR SMOOTH CURVE TRACE WITH ADIABATIC AND ISOTHERMAL LIMITS AND COMPRESSION AND EXPANSION STROKE PHASE DIFFERENCES

FIGURE 9

approach being perfectly adiabatic while the isothermal limit approaches a curve where the compression and expansion strokes are perfectly isothermal. The TSTR vs. SSTR plot has been drawn on a graph with axes of equal length so that the curve has not been mistakenly lengthened in either direction to give the false appearance of being more adiabatic or isothermal. Nevertheless, the trace seems to approach the adiabatic limit in the high temperature portion of the plot, while approaching the isothermal limit in the low temperature portion of the plot. On the compression stroke the trace becomes perfectly adiabatic at a point early in the stroke at $TSTR \approx .865$ ($T = 434^{\circ}R$). On the expansion stroke the trace also becomes perfectly adiabatic at a point early in the stroke at $TSTR \approx 1.15$ ($T = 644^{\circ}R$). At each of these two points that actual rate of heat transfer in the system through the cylinder walls equals zero.

The points of apparent zero rate of heat transfer occur at $T = T_{wall} = 539.2^{\circ}R$. The difference between these points and the points of actual zero rate of heat transfer is the phase difference. In both the compression and expansion strokes the phase difference is leading as the point of actual zero rate of heat transfer occurs prior to reaching the point of apparent zero rate of heat transfer. The actual phase differences can be computed to be:

compression stroke 45° leading
expansion stroke 64° leading

The actual system loss figures computed were:

PdV loss = -24.931 in-lb_f

TdS loss = -25.107 in-lb_f

Non-dimensional PdV loss = -0.0584

Non-dimensional TdS loss = -0.0588

In both the dimensional and non-dimensional cases, the PdV and TdS losses showed less than one percent difference.

CHAPTER V
DISCUSSION

V.A. Data Point Scatter

The scatter evident in the temperature vs. volume plots and particularly in the temperature vs. entropy plots deserves explanation. In these plots this scatter occurs primarily in the center section of the trace, away from the areas of minimum and maximum cylinder volume. At the upper and lower end portions of all the plots, the data points are generally packed tightly together in an orderly fashion. This is due to the fact that at the ends of the compression and expansion stroke, the piston is decelerating rapidly, halting abruptly and then again rapidly accelerating away from its extreme position. This stopping and starting motion requires a great deal of time to cover a small distance in comparison to the piston's much more rapid pace at the mid-stroke position of its travel. Because the data points are taken at equal time intervals, many more data points are taken at the extreme positions of the plots providing the tighter packing and the generally smoother appearance in those areas.

Near the mid-stroke positions of the cycle a different situation exists. Here the piston is moving much more rapidly relative to the velocity experienced at the extreme cylinder positions. Again as the data points are taken at equal time intervals, a greater distance should exist

between points on each trace near the mid-stroke position. This situation alone does not account for the scatter, but along with two other possible causes, the existence of the scatter can be better explained.

First, the Nicolet oscilloscope samples 2048 volume and 2948 pressure data points per scope storage cycle at equal time intervals between each point. The procedure of the scope is to sample one volume data point, wait the appropriate time interval and then sample one pressure data point, continuing in this manner until the storage cycle is full. The scope does not have the capability to sample pressure and volume simultaneously. Therefore the resulting pressure-volume data point pair formed by matching a volume data point with the following pressure data point does not exactly coincide with that pressure-volume data point pair that would occur if the capability existed to sample each pair simultaneously. This fact brings a small amount of error into the position of each data point.

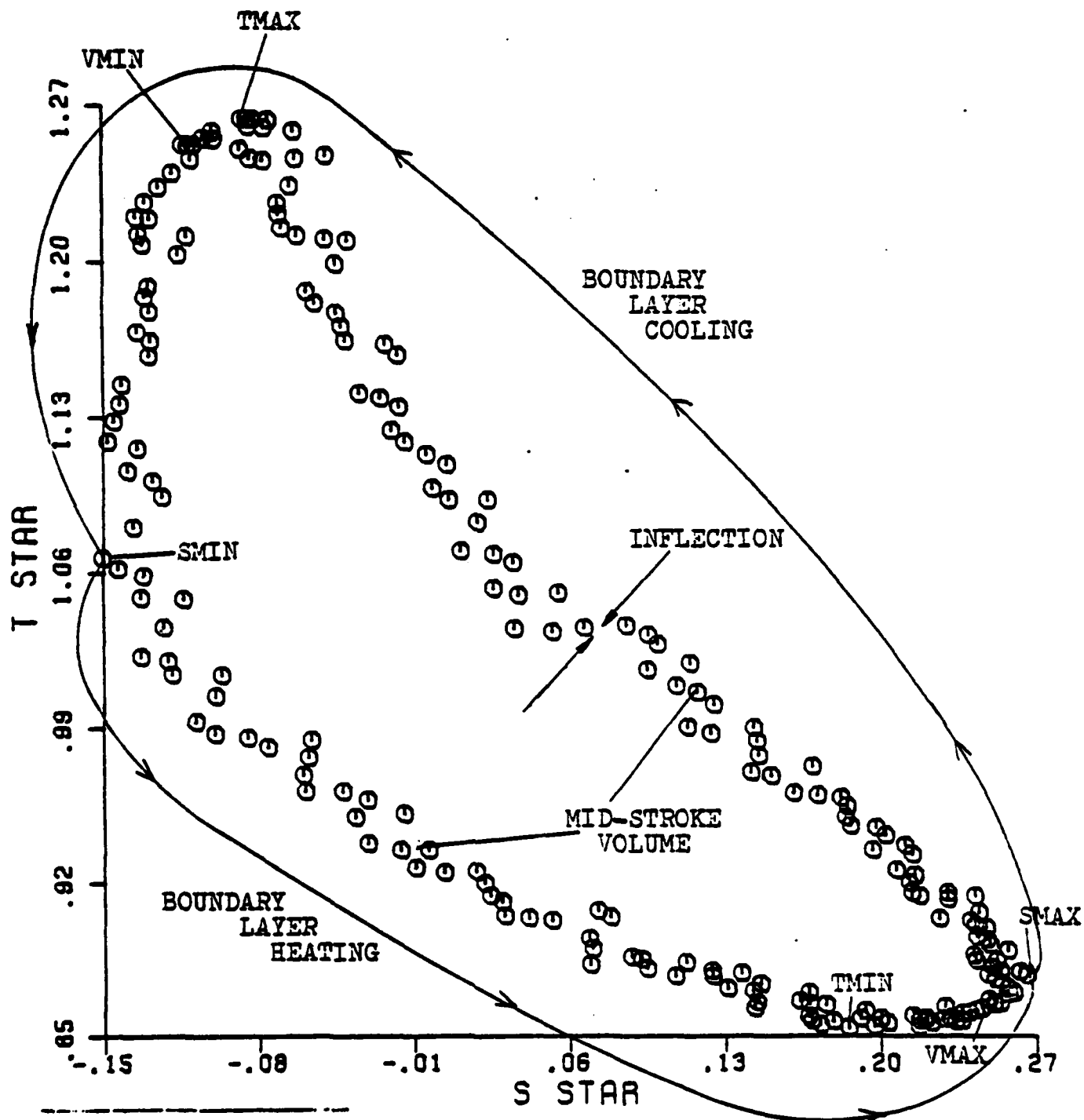
Second, the digital nature of the data generates additional error. The accuracy of the digital data output of the Nicolet was limited to .05 millivolt. With the large number of data points taken, the changes in output voltage between many points was less than .05 millivolt. Therefore voltage changes of less than .05 millivolt were rounded off to the next .05 millivolt increment creating some error in the data. This might have not been critical except for the

fact that the volume data was being read on the 100 millivolt scale on the oscilloscope, and the range of the data covered only 3.00 - 17.90 millivolts (roughly 15% of the range of the scale). The 100 millivolt scale was the best scale to use as it was the smallest scale available on the scope that would accept the range of the volume data. However, a 4X or 5X signal amplifier should have been connected in the volume signal wiring to utilize the full range of the 100 millivolt scale. This would have alleviated the problem existing due to the .05 millivolt accuracy of the Nicolet oscilloscope.

These limitations of the digital oscilloscope in conjunction with the magnitude of the mid-stroke piston velocity producing a greater distance between data points in this area of the plots, are surely a sufficient basis with which to attempt to justify the scatter.

V.B. Shape of Temperature vs. Entropy Plots

The actual shape of the temperature vs. entropy plots exhibits a few variations from what might be expected after seeing the other plots. In the high temperature end of the plot, the curve seems to approach its adiabatic limit, especially on the initial portion of the expansion stroke (Figure 10). The explanation for this is fairly simple. At the start of the expansion stroke, the temperature of the bulk gas and the temperature of the gas in the boundary layer are both greater than the cylinder wall temperature.



NON-DIMENSIONAL TEMPERATURE VS. NON-DIMENSIONAL ENTROPY PLOT ANNOTATED WITH MINIMUM AND MAXIMUM VALUES

FIGURE 10

However, the temperature of the bulk gas is still significantly greater than the boundary layer gas because the lower temperature cylinder wall has a greater effect on the temperature of the gas in the thin boundary layer. As the expansion stroke begins, the pressure drops and the bulk gas temperature drops rapidly. The temperature of the boundary layer gas drops also, but it drops at a much slower rate as it started the expansion stroke at a significantly lower temperature. Because the temperature difference between the boundary layer gas and the cylinder wall is not great for the first thirty degrees of the expansion stroke, very little heat is transferred out of the system and the process approaches its adiabatic limit.

At the low temperature end of the plot, near the end of the expansion stroke the curve seems to approach its isothermal limit (Figure 10). The explanation for this is very similar to that for the near adiabatic case. Near the end of the expansion stroke the boundary layer gas temperature has fallen somewhat lower than the cylinder wall temperature. In the last thirty degrees of the expansion stroke the volume in the cylinder increases, but it increases at a relative rate much less than the rate of increase near the start of the expansion stroke. Therefore the change in the bulk gas temperature will also change at a rate much less than the rate of change at the start of the expansion stroke. Even though the process approaches its isothermal limit,

there is still a sufficient temperature difference between the boundary layer gas and cylinder wall to permit significant heat transfer from the system.

The temperature vs. entropy plot also has what seems to be an inflection near the mid-stroke position on the compression stroke (Figure 10). At this inflection there is an abrupt change in the slope of the compression trace. Because of its proximity to the mid-stroke position on the curve, this inflection may be due to the change of piston acceleration to deceleration at mid-stroke. No such glaring inflection is evident in the expansion curve.

V.C. Identification of the Adiabatic Points in the Cycle

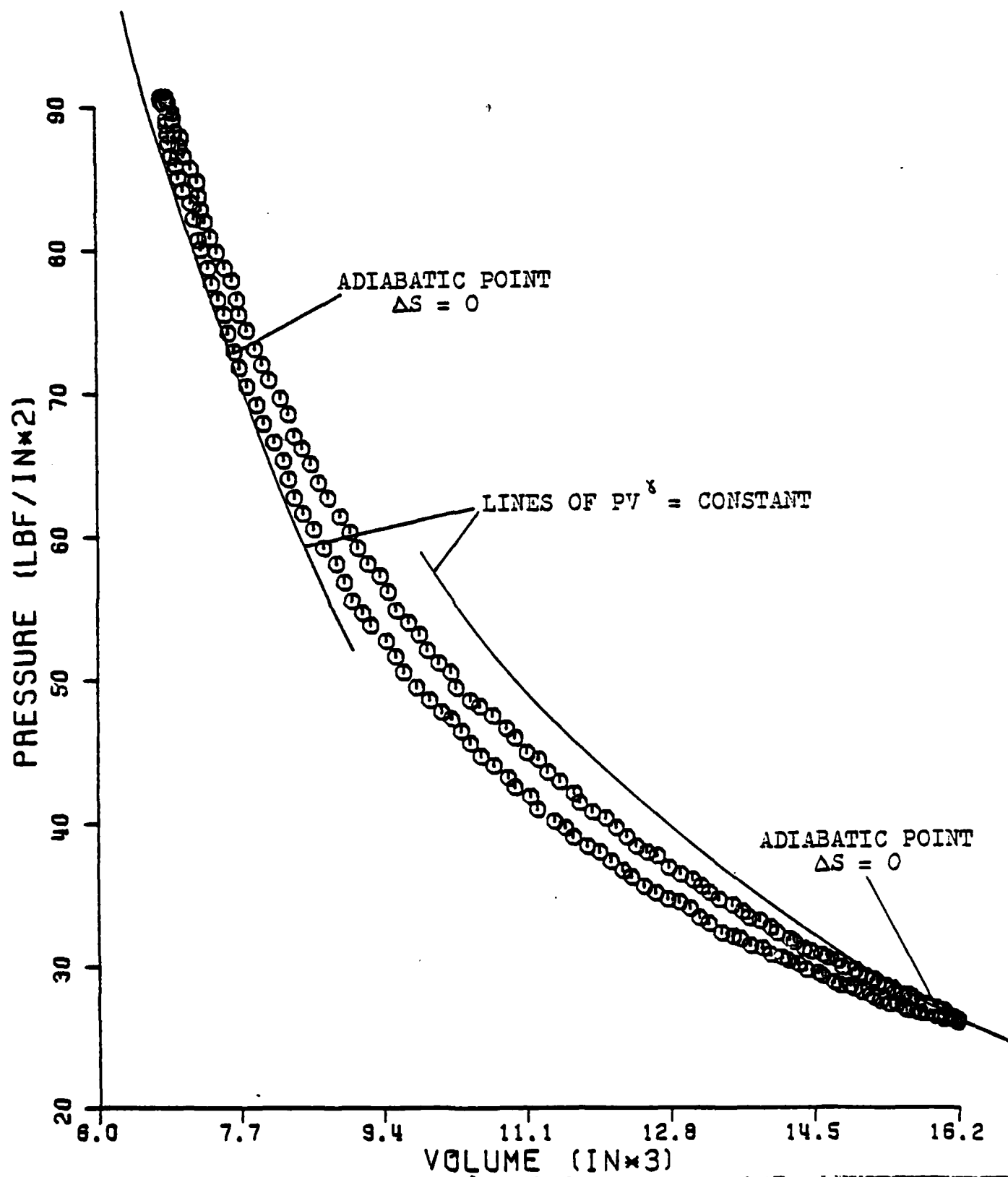
The identification of the two points in the cycle that are adiabatic is extremely important in determining the actual phase difference between the heat transfer and the bulk gas to wall temperature difference. It is expected that both the compression and expansion strokes should each have one adiabatic point where $T_{\text{boundary layer}} = T_{\text{wall}}$. Ideally this should occur at the points of maximum and minimum values of entropy. However, because of the scatter in the temperature vs. entropy plots it was difficult to envision the actual location where the curve became tangent to the vertical. Therefore to identify the location a rough curve was passed through the data points (Figure 9) and the adiabatic points were then evaluated at the locations where the curve passed through the vertical.

To check these adiabatic locations, lines of $PV^\gamma =$ constant (adiabatics) were constructed on the pressure vs. volume plot (Figure 11). The locations on the trace that were tangent to an adiabatic line would signify an adiabatic point. The results of this procedure verified the selection of the adiabatic points in Figure 9.

V.D. Effects of the Boundary Layer

The effects of the boundary layer on the rate of heat transfer, or more specifically on the losses in the system are most important. It is obvious that it is the temperature of the boundary layer gas and not the bulk gas temperature which is the driving force on the transfer of heat through the cylinder wall. If the boundary layer gas temperature is greater than the temperature of the cylinder wall, the system will lose heat. If the boundary layer gas temperature is less than the temperature of the cylinder wall, the system will gain heat.

Along the compression stroke and part of the expansion stroke from the minimum to maximum entropy value the boundary layer acts to cool the system (Figure 10). On this area of the curve the boundary layer gas temperature is basically greater than the cylinder wall temperature and heat will be transferred out of the system through the cylinder walls. The heat transfer in this portion of the curve is driven by the change in volume and not the change in the bulk gas temperature of the system.



PRESSURE VS. VOLUME PLOT WITH LINES OF $PV^\gamma = \text{CONSTANT}$

FIGURE 11

Along the expansion stroke from the minimum entropy value to the maximum entropy value the boundary layer acts to heat the system (Figure 10). The temperature of the bulk gas and the boundary layer is falling; however, the boundary layer temperature is generally less than the cylinder wall temperature and therefore heat will be transferred into the system through the cylinder walls.

V.E. Explanation of the Phase Difference

The phase difference that exists in the zero rate of heat transfer location is a very important effect of the boundary layer (Figure 9). The explanation of the cause for the phase difference should be fully discussed.

The bulk gas temperature is an important parameter in this type of system. Because the bulk gas temperature is much easier to measure and to understand than the more difficult to measure boundary layer temperature, the bulk gas temperature is utilized much more in this type of system. Therefore, if the bulk gas temperature is utilized, then when deriving the apparent expression that would define the rate of heat transfer from the system, the temperature extremes utilized would be the bulk gas temperature and the cylinder wall temperature and the expression would be:

$$q = hA (T_{\text{bulk gas}} - T_{\text{wall}}).$$

For this expression the points of zero rate of heat transfer are the points on the cycle where $T_{\text{bulk gas}} = T_{\text{wall}}$.

The existence of a boundary layer with finite heat capacitance alters the former interpretation of the problem. The temperature of the gas in the layer next to the cylinder wall will not equal the bulk gas temperature, but will equal the boundary layer gas temperature. Therefore, the expression defining the rate of heat transfer to the cylinder walls will become:

$$q = hA (T_{\text{boundary layer}} - T_{\text{wall}}).$$

This expression specifies that the points of zero rate of heat transfer would be the points on the cycle where $T_{\text{boundary layer}} = T_{\text{wall}}$. Because the bulk gas temperature is not equal to the boundary layer gas temperature in this system, some difference will exist in the time of apparent zero rate of heat transfer and actual zero rate of heat transfer. This difference is the zero rate of heat transfer phase difference. The phase difference in both the compression and expansion strokes of this experimentation was leading, or the actual zero rate of heat transfer occurred in the cycle before the apparent zero rate of heat transfer (Figure 9).

The explanation for the phase difference exists in the examination of the temperature history of the boundary layer. As the compression stroke is started the boundary layer gas temperature is slightly greater than the bulk gas temperature. This is due to the fact that the cylinder wall temperature is

greater than the bulk gas temperature and the cylinder wall temperature has a much greater effect on the temperature of the boundary layer gas rather than the bulk gas. As the gas is compressed the bulk gas and boundary layer gas temperatures rise, but because the boundary layer gas temperature started the stroke at a higher temperature than the bulk gas, the boundary layer gas temperature passes through the cylinder wall temperature prior to the bulk gas providing a leading phase difference.

As the expansion stroke is started both the bulk gas and boundary layer gas are cooled by the drop in pressure. But because the boundary layer gas temperature was significantly lower than the bulk gas temperature at the beginning of the expansion stroke, the boundary layer gas temperature passes through the cylinder wall temperature prior to the bulk gas providing a leading phase difference.

CHAPTER VI
CONCLUSIONS

One of the original objectives of the work included the capability of direct transmission of the data from the experimental expander to the Institute's CMS computer system. This capability required the use of a converter that could properly interface with the Nicolet storage oscilloscope and the CMS computer system. The Electric Power Systems Laboratory was assigned the task of designing and assembling this interface unit. Due to manpower shortages, the Electric Power Systems Laboratory was not able to complete the assembly of the interface unit prior to the submission of this paper. The unavailability of the interface unit required the data to be read point by point digitally from the Nicolet storage oscilloscope and then manually entered into a CMS computer system data file.

With the use of an operable interface unit, dozens of cycle runs could have been performed. However, the lack of the interface significantly limited the number of cycle runs that could be evaluated. Further setbacks occurred when serious problems were encountered in the digital and graphic data presentation from the Nicolet storage oscilloscope. The final result was the availability of only one good set of cycle data for analysis.

Although the technique developed in this paper to analyze the data was used on only one set of experimental

data, the results obtained proved that the analysis method was highly credible. Whether one or one hundred sets of cycle data had been evaluated, the same method would have been utilized.

The additional runs that could have been performed with an operable interface unit would have greatly increased the scope of the experiment. Parameters such as piston RPM, Reynold's number, cylinder volume ratio, cylinder pressure and type of working gas could have been varied. The results that would have been presented with the variations in the above parameters would have provided insight into the actual heat transfer losses and phase difference for a wide range of conditions. This general information could then be extrapolated for use in the design of other devices of this type.

REFERENCES

1. Bell, J. H. Jr., Cryogenic Engineering, Prentice-Hall, Inc., Englewood Cliffs, New Jersey, 1963.
2. Frost, Walter, Heat Transfer at Low Temperatures, The International Cryogenic Monograph Series, Plenum Press, New York, 1975.
3. Goetz, Theodore E., "An Experimental Investigation of Work Losses Due to Non-Adiabatic Gas Expansion", M.I.T. Department of Mechanical Engineering Bachelor of Science Thesis, May 1977.
4. McClintock, Michael, Cryogenics, Reinhold Publishing Corp., New York, 1964.
5. Rohsenow, Warren M. and Harry Y. Choi, Heat, Mass, and Momentum Transfer, Prentice-Hall, Inc., Englewood Cliffs, New Jersey, 1961.
6. Scott, Russell B., Cryogenic Engineering, Van Nostrand Company, Inc., Princeton, New Jersey, 1959.
7. Vance, Robert W., ed. Cryogenic Technology, Wiley and Sons, New York, 1963.
8. Wark, Kenneth, Thermodynamics, McGraw-Hill, Inc., New York, 1971.

APPENDIX A

CYCLE FORTRAN PROGRAM LISTING

CYCLE PROGRAM LISTING

CYC00010
 CYC00020
 CYC00030
 CYC00040
 CYC00050
 CYC00060
 CYC00070
 CYC00080
 CYC00090
 CYC00100
 CYC00110
 CYC00120
 CYC00130
 CYC00140
 CYC00150
 CYC00160
 CYC00170
 CYC00180
 CYC00190
 CYC00200
 CYC00210
 CYC00220
 CYC00230
 CYC00240
 CYC00250
 CYC00260
 CYC00270
 CYC00280
 CYC00290
 CYC00300
 CYC00310
 CYC00320
 CYC00330
 CYC00340
 CYC00350
 CYC00360
 CYC00370
 CYC00380
 CYC00390
 CYC00400
 CYC00410

```

10 DIMENSION P(230), V(230), PR(230), VOL(230), T(230), S(230),
    IPSTR(230), VSTR(230), TSIR(230), SSIR(230)
    READ (32,10) (P(I), V(I), I=1,225)
    FORMAT (10X, F6.2, F8.3)
    R=386.33
    CP=1.25
    CV=.75
    VTDC=6.77
    VBDC=16.19
    DISP=VBDC-VTDC
    RPH=267.0
    TINT=1.0
    TO=559.67
    THR1=26.8
    THR2=26.0
    THR3=26.4
    THR4=25.7
    TVAL=((THR1+THR2+THR3)*1.8)/3. )+32. G+459.67
    VMAX=V(1)
    VMIN=V(1)
    NMAX=1
    NMIN=1
    M=225
    MM1=M-1
    DO 40 I=1,MM1
    IF(VMAX.GT. V(I+1)) GO TO 35
    VMAX=V(I+1)
    NMAX=I+1
35 IF (VMIN .LT. V(I+1)) GO TO 40
    VMIN=V(I+1)
    NMIN=I+1
40 CONTINUE
    DO 50 I=1,M
    P(I)=(P(I)-.4)*4.342+14.7
    V(I)=((V(I)-VMIN)/(VMAX-VMIN))*(VBDC-VTDC)+VTDC
50 CONTINUE
    I1=1
    JMM1=M+NMAX-1
    DO 60 J=NMAX, JMM1
    JJ=J
    IF (J .GT. M) JJ=J-M
  
```

```

CYC000420
CYC000430
CYC000440
CYC000450
CYC000460
CYC000470
CYC000480
CYC000490
CYC000500
CYC000510
CYC000520
CYC000530
CYC000540
CYC000550
CYC000560
CYC000570
CYC000580
CYC000590
CYC000600
CYC000610
CYC000620
CYC000630
CYC000640
CYC000650
CYC000660
CYC000670
CYC000680
CYC000690
CYC000700
CYC000710
CYC000720
CYC000730
CYC000740
CYC000750
CYC000760
CYC000770
CYC000780
CYC000790
CYC000800
CYC000810
CYC000820
CYC000830
CYC000840
CYC000850
CYC000860
CYC000870

IF (J .EQ. MMIN) MMIN=I+1
VOL(I)=V(JJ)
PR(I)=P(JJ)
I=I+1
CONTINUE
DO 90 I=1,M
V0=(SQRT(VBDC/VTDC))*VTDC
IF (I .EQ. M) VOL(I+1)=VOL(I)
IF (I .EQ. M) PR(I+1)=PR(I)
IF (VOL(I) .GE. V0) GO TO 75
IF (VOL(I) .LE. V0) GO TO 76
IF (VOL(I+1) .LE. V0) GO TO 80
GO TO 90
IF (VOL(I+1) .GE. V0) GO TO 85
GO TO 90
PHI=PR(I+1)-((V0-VOL(I+1))*(PR(I+1)-PR(I))/(VOL(I)-VOL(I+1)))
GO TO 90
PLOW=PR(I+1)+((V0-VOL(I+1))*(PR(I)-PR(I+1))/(VOL(I)-VOL(I+1)))
CONTINUE
PO=(PHI+PLOW)/2.
TMAS=PO*V0/(R*TO*12)
MPDV=0.
MC=0.
ME=0.
DO 100 I=1,M
VOL(I+1)=VOL(I)
IF (I .EQ. M) PR(I+1)=PR(I)
IF (VOL(I+1) .GT. VOL(I)) GO TO 95
MC=MC+PR(I)*(VOL(I)-VOL(I+1))*(PR(I+1)-PR(I))*(VOL(I)-VOL(I+1))/
12.
GO TO 100
95 ME=ME+PR(I)*(VOL(I)-VOL(I+1))*(PR(I+1)-PR(I))*(VOL(I)-VOL(I+1))/
12.
CONTINUE
MPDV=ME+MC
DO 110 I=1,M
T(I)={PR(I)*VOL(I)}/(R*TMAS*12.)
S(I)=TMAS*12.*(CV*ALOG(PR(I)/PO)+CP*ALOG(VOL(I)/V0))
CONTINUE
PMEP=MC/DISP
DO 120 I=1,M
VSTR(I)=VOL(I)/DISP
PSTR(I)=PR(I)/PMEP
TSTR(I)=T(I)/TO
SSTR(I)=S(I)*TO/(PMEP*DISP)
CONTINUE
MTDS=0.
MPST=0.
60
75
76
80
85
90
95
100
110
120

```

```

CYC00660
CYC00690
CYC00900
CYC00910
CYC00920
CYC00930
CYC00940
CYC00950
CYC00960
CYC00970
CYC00980
CYC00990
CYC01000
CYC01010
CYC01020
CYC01030
CYC01040
CYC01050
CYC01060
MILLCYC01070

CYC01090
CYC01100
CYC01110
CYC01120
CYC01130
CYC01140
CYC01150
CYC01160
CYC01170
CYC01180
CYC01190
CYC01200
CYC01210
CYC01220
CYC01230
CYC01240
CYC01250
CYC01260
CYC01270
CYC01280
CYC01290
CYC01300
CYC01310
CYC01320
CYC01330
CYC01340
CYC01350

WIST=0.
DO 130 I=1,M
  T(I+1)=T(I)
  IF (.EQ. M) S(I+1)=S(I)
  IF (.EQ. M) VSTR(I+1)=VSTR(I)
  IF (.EQ. M) PSIR(I+1)=PSIR(I)
  IF (.EQ. M) TSTR(I+1)=TSTR(I)
  IF (.EQ. M) SSIR(I+1)=SSIR(I)
  WDS=WDS+T(I)*(S(I)-S(I+1))+T(I+1)-T(I))*(S(I)-S(I+1))/2.
  WPST=WPST+PSIR(I)*(S(I)-S(I+1))+VSTR(I)-VSTR(I+1)-PSIR(I))*
  1(VSTR(I)-VSTR(I+1))/2.
  WIST=WIST+TSTR(I)*(SSIR(I)-SSIR(I+1))+TSTR(I+1)-TSTR(I))*
  1(SSIR(I)-SSIR(I+1))/2.
CONTINUE
130 WRITE (6,190)
190 FORMAT (10,5X,'THE WORKING GAS IS HELIUM')
191 FORMAT (10,5X,'RPM = ',F6.1)
192 WRITE (6,192) TIM
192 FORMAT (10,5X,'TIME INTERVAL BETWEEN DATA POINTS = ',F3.1,' MILLCYC01070

130 WRITE (6,200) DISP
200 FORMAT (10,5X,'CYLINDER DISPLACEMENT = ',F5.3,' IN*3')
201 WRITE (6,201) P0
201 FORMAT (10,5X,'REFERENCE PRESSURE = ',F6.3,' LBF/IN*2')
202 WRITE (6,202) V0
202 FORMAT (10,5X,'REFERENCE VOLUME = ',F5.2,' IN*3')
203 WRITE (6,203) T0
203 FORMAT (10,5X,'REFERENCE TEMPERATURE = ',F5.2,' DEG R')
204 WRITE (6,204) TWAL
204 FORMAT (10,5X,'CYLINDER WALL TEMPERATURE = ',F6.2,' DEG R')
205 WRITE (6,205) TMAS
205 FORMAT (10,5X,'SYSTEM MASS = ',E10.4,' LBM')
206 WRITE (6,206) WPDV
206 FORMAT (10,5X,'PDV LOSS = ',F7.3,' IN-LBF')
207 WRITE (6,207) WIDS
207 FORMAT (10,5X,'TDS LOSS = ',F7.3,' IN-LBF')
208 WRITE (6,208) WPST
208 FORMAT (10,5X,'NON-DIMENSIONAL PDV LOSS = ',F7.4)
209 WRITE (6,209) WIST
209 FORMAT (10,5X,'NON-DIMENSIONAL TDS LOSS = ',F7.4)
210 WRITE (6,210)
210 FORMAT (10,2X,'1',3X,'PRES',4X,'VOL',4X,'TEMP',5X,'ENTR',5X,
1'PSTR',4X,'VSTR',4X,'TSTR',5X,'SSIR')
211 WRITE (6,211) (I,PR(I),VOL(I),T(I),S(I),PSIR(I),VSTR(I),TSTR(I),
1SSIR(I),I=1,M)
212 FORMAT (2X,13,F8.3,F7.2,F8.2,F10.5,3F8.4,F10.5)
CALL PLOTS (IDUM, IDUM, 20)

```

```

CYC01360
CYC01370
CYC01380
CYC01390
CYC01400
CYC01410
CYC01420
CYC01430
CYC01440
CYC01450
CYC01460
CYC01470
CYC01480
CYC01490
CYC01500
CYC01510
CYC01520
CYC01530
CYC01540
CYC01550
CYC01560
CYC01570
CYC01580
CYC01590

CYC01610
CYC01620
CYC01630
CYC01640
CYC01650
CYC01660
CYC01670
CYC01680
CYC01690
CYC01700
CYC01710
CYC01720
CYC01730
CYC01740
CYC01750
CYC01760
CYC01770

CALL PVPL0T (PR,VOL,M)
CALL TVPL0T (T,VOL,M)
CALL TSPLOT (T,S,M)
CALL NDPVPL (PSTR,VSIR,M)
CALL NDTVPL (TSIR,VSIR,M)
CALL NDISPL (TSIR,SSIR,M)
CALL ENDPLOT (7.0,0.0,999)
STOP
END
SUBROUTINE PVPL0T (PP,VV,NPT)
DIMENSION PP(230),VV(230)
CALL PICTUR (6.0,7.0,'VOLUME (IN*3)',13,'PRESSURE (LBF/IN*2)',19,
1VV,PP,-NPT,.1,1)
RETURN
END
SUBROUTINE TVPL0T (TT,VV,NPT)
DIMENSION TT(230),VV(230)
CALL PICTUR (6.0,7.0,'VOLUME (IN*3)',13,'TEMPERATURE (DEG R)',19,
1VV,TT,-NPT,.1,1)
RETURN
END
SUBROUTINE TSPLOT (TT,SS,NPT)
DIMENSION TT(230),SS(230)
CALL PICTUR (6.0,7.0,'ENTROPY (IN-LBF/DEG R)',22,'TEMPERATURE (DEG R)',19,
1G R',19,SS,TT,-NPT,.1,1)
RETURN
END
SUBROUTINE NDPVPL (PPST,VVST,NPT)
DIMENSION PPST(230),VVST(230)
CALL PICTUR (6.0,7.0,'V STAR',6,'P STAR',6,'VVST,PPST,-NPT,.1,1)
RETURN
END
SUBROUTINE NDTVPL (TTST,VVST,NPT)
DIMENSION TTST(230),VVST(230)
CALL PICTUR (6.0,7.0,'V STAR',6,'T STAR',6,'VVST,TTST,-NPT,.1,1)
RETURN
END
SUBROUTINE NDISPL (TTST,SSST,NPT)
DIMENSION TTST(230),SSST(230)
CALL PICTUR (6.0,6.0,'S STAR',6,'T STAR',6,'SSST,TTST,-NPT,.1,1)
RETURN
END

```

APPENDIX B

CYCLE DATA FILE LISTING

PRINTOUT OF THE DATA FILE

PRESSURE READINGS IN MILLIVOLTS
VOLUME READINGS IN VOLTS

PRESS	VOLUME
8.65	-2.560
8.40	-2.540
8.20	-2.485
8.10	-2.450
7.95	-2.400
7.75	-2.350
7.60	-2.315
7.35	-2.270
7.25	-2.225
7.05	-2.190
6.90	-2.145
6.70	-2.090
6.55	-2.070
6.40	-2.020
6.30	-1.970
6.15	-1.930
6.00	-1.890
5.85	-1.855
5.75	-1.815
5.70	-1.775
5.50	-1.730
5.40	-1.685
5.30	-1.640
5.20	-1.605
5.10	-1.575
5.00	-1.540
4.90	-1.490
4.80	-1.450
4.70	-1.425
4.65	-1.385
4.55	-1.345
4.45	-1.320
4.35	-1.270
4.30	-1.255
4.20	-1.215
4.15	-1.190
4.10	-1.150

4.05	-1.130
4.00	-1.090
3.90	-1.075
3.85	-1.025
3.80	-1.010
3.75	-.985
3.70	-.955
3.65	-.940
3.60	-.910
3.55	-.885
3.50	-.875
3.45	-.850
3.40	-.825
3.35	-.810
3.30	-.790
3.30	-.770
3.25	-.760
3.25	-.740
3.25	-.720
3.25	-.720
3.20	-.710
3.20	-.690
3.15	-.680
3.05	-.675
3.10	-.670
3.10	-.655
3.05	-.650
3.10	-.650
3.05	-.650
3.05	-.635
3.00	-.640
3.00	-.645
3.05	-.640
3.05	-.640
3.05	-.640
3.05	-.660
3.05	-.655
3.05	-.650
3.05	-.665
3.05	-.675
3.05	-.680
3.05	-.690
3.05	-.700
3.10	-.720
3.10	-.725
3.15	-.730
3.15	-.755
3.15	-.775

3.15	- .765
3.20	- .805
3.25	- .830
3.30	- .845
3.30	- .865
3.30	- .890
3.35	- .900
3.40	- .955
3.45	- .965
3.50	- 1.000
3.55	- 1.030
3.60	- 1.045
3.60	- 1.085
3.65	- 1.105
3.75	- 1.150
3.80	- 1.165
3.85	- 1.210
3.95	- 1.240
4.00	- 1.280
4.05	- 1.300
4.10	- 1.345
4.20	- 1.375
4.25	- 1.420
4.35	- 1.460
4.40	- 1.485
4.45	- 1.530
4.60	- 1.580
4.70	- 1.615
4.85	- 1.650
4.95	- 1.690
5.00	- 1.735
5.10	- 1.780
5.20	- 1.825
5.35	- 1.870
5.45	- 1.905
5.60	- 1.950
5.75	- 1.995
5.85	- 2.040
6.00	- 2.095
6.15	- 2.125
6.25	- 2.165
6.45	- 2.230
6.65	- 2.255
6.80	- 2.315
6.95	- 2.340
7.15	- 2.395
7.30	- 2.445

7.50 -2.485
7.70 -2.520
7.90 -2.555
8.00 -2.595
8.20 -2.640
8.40 -2.690
8.65 -2.740
8.90 -2.770
9.15 -2.805
9.40 -2.865
9.60 -2.895
9.80 -2.935
10.10 -2.965
10.40 -2.995
10.65 -3.045
10.95 -3.080
11.20 -3.120
11.45 -3.155
11.75 -3.175
12.05 -3.195
12.35 -3.230
12.65 -3.270
12.95 -3.295
13.25 -3.335
13.55 -3.360
13.80 -3.380
14.10 -3.405
14.40 -3.420
14.65 -3.440
14.90 -3.465
15.15 -3.480
15.45 -3.505
15.60 -3.515
15.95 -3.530
16.20 -3.545
16.40 -3.575
16.60 -3.590
16.80 -3.600
16.95 -3.615
17.15 -3.625
17.30 -3.630
17.45 -3.635
17.55 -3.635
17.75 -3.640
17.80 -3.650
17.85 -3.655
17.90 -3.660
17.90 -3.650

17.05	-3.650
17.90	-3.640
17.85	-3.635
17.80	-3.630
17.70	-3.625
17.65	-3.615
17.55	-3.610
17.35	-3.605
17.25	-3.580
17.10	-3.585
16.95	-3.570
16.75	-3.545
16.55	-3.520
16.30	-3.515
16.10	-3.505
15.90	-3.490
15.65	-3.470
15.40	-3.445
15.15	-3.415
14.95	-3.390
14.65	-3.370
14.40	-3.360
14.15	-3.335
13.85	-3.300
13.60	-3.275
13.35	-3.250
13.05	-3.205
12.80	-3.175
12.45	-3.155
12.25	-3.125
12.00	-3.090
11.70	-3.060
11.45	-3.025
11.15	-2.980
10.90	-2.940
10.65	-2.915
10.40	-2.875
10.20	-2.830
9.95	-2.800
9.65	-2.765
9.45	-2.720
9.25	-2.680
9.00	-2.650
8.80	-2.605

APPENDIX C

CYCLE PROGRAM DATA OUTPUT

PRINTOUT OF CYCLE PROGRAM PARAMETERS

THE WORKING GAS IS HELIUM

RPM = 267.0

TIME INTERVAL BETWEEN DATA POINTS = 1.0 MILLISEC

CYLINDER DISPLACEMENT = 9.420 IN³

REFERENCE PRESSURE = 46.827 LBF/IN²

REFERENCE VOLUME = 10.47 IN³

REFERENCE TEMPERATURE = 559.67 DEG R

CYLINDER WALL TEMPERATURE = 539.19 DEG R

SYSTEM MASS = 0.1889E-03 LBM

PDV LOSS = -24.931 IN-LBF

TDS LOSS = -25.107 IN-LBF

NON-DIMENSIONAL PDV LOSS = -0.0584

NON-DIMENSIONAL TDS LOSS = -0.0588

PRINTOUT OF CYCLE PROGRAM DATA

	PRES	VOL	TEMP	ENTR	PSIR	VSIR	TSIR	SSIR
1	26.206	16.19	484.36	0.19331	0.5785	1.7187	0.8654	0.23351
2	25.989	16.17	479.89	0.18018	0.5737	1.7170	0.8574	0.23630
3	25.989	16.16	479.42	0.17806	0.5737	1.7154	0.8566	0.23351
4	26.206	16.17	483.89	0.19119	0.5785	1.7170	0.8646	0.25073
5	26.206	16.17	483.89	0.19119	0.5785	1.7170	0.8646	0.25073
6	26.206	16.11	482.03	0.18268	0.5785	1.7104	0.8613	0.23957
8	26.206	16.13	482.50	0.18481	0.5785	1.7121	0.8621	0.24237
9	26.206	16.14	482.96	0.18694	0.5785	1.7137	0.8629	0.24516

10	26.206	16.10	481.57	0.18055	0.5785	1.7088	0.8604	0.23678
11	26.206	16.07	480.63	0.17628	0.5785	1.7055	0.8580	0.23118
12	26.206	16.05	480.17	0.17414	0.5785	1.7038	0.8579	0.22837
13	26.206	16.02	479.24	0.16986	0.5785	1.7005	0.8563	0.22276
14	26.206	15.99	478.30	0.16557	0.5785	1.6972	0.8546	0.21713
15	26.423	15.93	480.39	0.16788	0.5833	1.6906	0.8583	0.22016
16	26.423	15.91	479.92	0.16572	0.5833	1.6889	0.8575	0.21733
17	26.640	15.89	483.39	0.17439	0.5880	1.6873	0.8637	0.22870
18	26.640	15.82	481.02	0.16356	0.5880	1.6790	0.8595	0.21450
19	26.640	15.75	479.13	0.15486	0.5880	1.6724	0.8561	0.20309
20	26.640	15.72	478.18	0.15050	0.5880	1.6691	0.8544	0.19737
21	26.858	15.66	480.17	0.15248	0.5928	1.6625	0.8579	0.19997
22	26.858	15.58	477.78	0.14149	0.5928	1.6542	0.8537	0.18556
23	27.075	15.54	480.20	0.14553	0.5976	1.6493	0.8580	0.19085
24	27.292	15.47	482.11	0.14723	0.6024	1.6426	0.8614	0.19309
25	27.292	15.40	479.68	0.13611	0.6024	1.6344	0.8571	0.17850
26	27.292	15.36	478.71	0.13165	0.6024	1.6311	0.8553	0.17265
27	27.509	15.27	479.59	0.12868	0.6072	1.6212	0.8569	0.16876
28	27.726	15.19	480.91	0.12781	0.6120	1.6129	0.8593	0.16762
29	27.943	15.16	483.68	0.13361	0.6168	1.6096	0.8642	0.17522
30	28.160	15.05	483.93	0.12794	0.6216	1.5980	0.8647	0.16778
31	28.377	14.96	484.64	0.12437	0.6264	1.5881	0.8659	0.16311
32	28.594	14.91	486.82	0.12756	0.6312	1.5831	0.8698	0.16729
33	28.594	14.79	482.75	0.10907	0.6312	1.5699	0.8626	0.14303
34	28.811	14.73	484.37	0.10977	0.6360	1.5633	0.8655	0.14395
35	29.246	14.59	486.99	0.10847	0.6455	1.5484	0.8701	0.14226
36	29.463	14.54	489.04	0.11119	0.6503	1.5435	0.8738	0.14581
37	29.680	14.40	487.89	0.09954	0.6551	1.5286	0.8717	0.13055
38	30.114	14.31	491.82	0.10441	0.6647	1.5187	0.8788	0.13692
39	30.331	14.18	491.05	0.09463	0.6695	1.5055	0.8774	0.12410
40	30.548	14.12	492.39	0.05436	0.6743	1.4988	0.8798	0.12374
41	30.765	13.98	490.97	0.08173	0.6791	1.4840	0.8773	0.10719
42	31.200	13.89	494.57	0.08549	0.6887	1.4741	0.8837	0.11211
43	31.417	13.75	492.99	0.07230	0.6935	1.4592	0.8809	0.09481
44	31.851	13.62	495.27	0.07038	0.7031	1.4460	0.8849	0.09230
45	32.068	13.54	495.80	0.06673	0.7078	1.4377	0.8859	0.08751
46	32.285	13.40	493.99	0.05272	0.7126	1.4228	0.8826	0.06914
47	32.936	13.25	498.10	0.05338	0.7270	1.4063	0.8900	0.07001
48	33.371	13.14	500.52	0.05249	0.7366	1.3947	0.8943	0.06884
49	34.022	13.03	506.05	0.05929	0.7606	1.3699	0.9070	0.07251
50	34.456	12.90	507.61	0.05529	0.7654	1.3550	0.9028	0.05184
51	34.673	12.76	505.26	0.03953	0.7749	1.3402	0.9041	0.04151
52	35.107	12.62	505.97	0.03165	0.7845	1.3253	0.9051	0.03056
53	35.542	12.48	506.54	0.02330	0.7989	1.3104	0.9113	0.02942
54	36.193	12.34	510.04	0.02243	0.7989	1.3104	0.9113	0.02942
55	36.627	12.24	511.60	0.01866	0.8085	1.2988	0.9141	0.02447
56	37.278	12.10	514.73	0.01657	0.8229	1.2840	0.9197	0.02174
57	37.930	11.95	517.66	0.01379	0.8372	1.2691	0.9249	0.01809

58	38.364	11.81	517.44	0.00285	0.8468	1.2542	0.9246	0.00374
59	39.015	11.64	518.60	-0.00707	0.8612	1.2360	0.9266	-0.00928
60	39.666	11.55	523.03	-0.00293	0.8756	1.2261	0.9345	-0.00385
61	40.101	11.43	523.05	-0.01244	0.8852	1.2129	0.9346	-0.01631
62	40.969	11.22	524.91	-0.02351	0.9043	1.1914	0.9379	-0.03083
63	41.837	11.15	532.32	-0.01111	0.9235	1.1831	0.9511	-0.01457
64	42.489	10.96	531.54	-0.02795	0.9379	1.1633	0.9497	-0.03666
65	43.140	10.88	535.86	-0.02355	0.9522	1.1550	0.9575	-0.03088
66	44.008	10.71	538.04	-0.03216	0.9714	1.1369	0.9614	-0.04218
67	44.660	10.55	538.06	-0.04502	0.9858	1.1203	0.9614	-0.05904
68	45.528	10.43	542.05	-0.04572	1.0050	1.1071	0.9685	-0.05996
69	46.397	10.32	546.62	-0.04389	1.0241	1.0955	0.9767	-0.05756
70	47.265	10.21	550.97	-0.04277	1.0433	1.0840	0.9844	-0.05609
71	47.699	10.09	549.25	-0.05773	1.0529	1.0707	0.9814	-0.07572
72	48.568	9.95	551.46	-0.06471	1.0720	1.0559	0.9854	-0.08487
73	49.436	9.79	552.55	-0.07606	1.0912	1.0393	0.9873	-0.09974
74	50.521	9.63	555.70	-0.07603	1.1152	1.0228	0.9929	-0.10842
75	51.607	9.54	562.14	-0.07382	1.1391	1.0129	1.0044	-0.09971
76	52.692	9.43	567.40	-0.09096	1.1631	0.9815	1.0138	-0.09681
77	53.778	9.25	567.62	-0.09216	1.1871	0.9615	1.0142	-0.11929
78	54.646	9.15	570.96	-0.09216	1.2062	0.9716	1.0202	-0.12087
79	55.515	9.03	572.14	-0.10152	1.2254	0.9584	1.0223	-0.13314
80	56.817	8.93	579.50	-0.09377	1.2541	0.9484	1.0354	-0.12298
81	58.120	8.84	586.59	-0.08696	1.2829	0.9385	1.0481	-0.11404
82	59.205	8.69	587.02	-0.10166	1.3069	0.9220	1.0489	-0.13332
83	60.508	8.58	592.41	-0.10071	1.3356	0.9104	1.0585	-0.13208
84	61.594	8.45	594.28	-0.10945	1.3596	0.8972	1.0618	-0.14354
85	62.679	8.34	596.95	-0.11496	1.3835	0.8856	1.0666	-0.15076
86	63.982	8.28	604.81	-0.10427	1.4123	0.8790	1.0807	-0.13674
87	65.284	8.22	612.48	-0.09425	1.4410	0.8724	1.0944	-0.12361
88	66.587	8.11	616.42	-0.09755	1.4698	0.8608	1.1014	-0.12794
89	67.889	7.98	618.82	-0.10606	1.4985	0.8476	1.1057	-0.13909
90	69.192	7.91	624.55	-0.10252	1.5273	0.8393	1.1159	-0.13444
91	70.495	7.78	626.28	-0.11286	1.5560	0.8261	1.1190	-0.14800
92	71.797	7.70	631.47	-0.11080	1.5848	0.8179	1.1283	-0.14531
93	72.883	7.64	635.84	-0.10885	1.6088	0.8112	1.1361	-0.14275
94	74.185	7.56	640.61	-0.10799	1.6375	0.8030	1.1446	-0.14162
95	75.488	7.52	647.83	-0.09862	1.6663	0.7980	1.1575	-0.12933
96	76.573	7.46	651.70	-0.09808	1.6902	0.7914	1.1644	-0.12862
97	77.659	7.38	654.04	-0.10260	1.7142	0.7831	1.1686	-0.13455
98	78.744	7.33	658.98	-0.09824	1.7381	0.7782	1.1774	-0.12884
99	80.047	7.25	662.77	-0.10008	1.7669	0.7699	1.1842	-0.13125
100	80.698	7.22	665.29	-0.09884	1.7813	0.7666	1.1887	-0.12963
101	82.218	7.17	673.43	-0.08847	1.8148	0.7617	1.2033	-0.11602
102	83.304	7.13	677.88	-0.08552	1.8388	0.7567	1.2112	-0.11215
103	84.172	7.03	675.97	-0.10089	1.8580	0.7468	1.2078	-0.13231
104	85.040	6.99	678.41	-0.10200	1.8771	0.7418	1.2122	-0.13377
105	85.909	6.96	682.29	-0.09841	1.8963	0.7385	1.2191	-0.12906

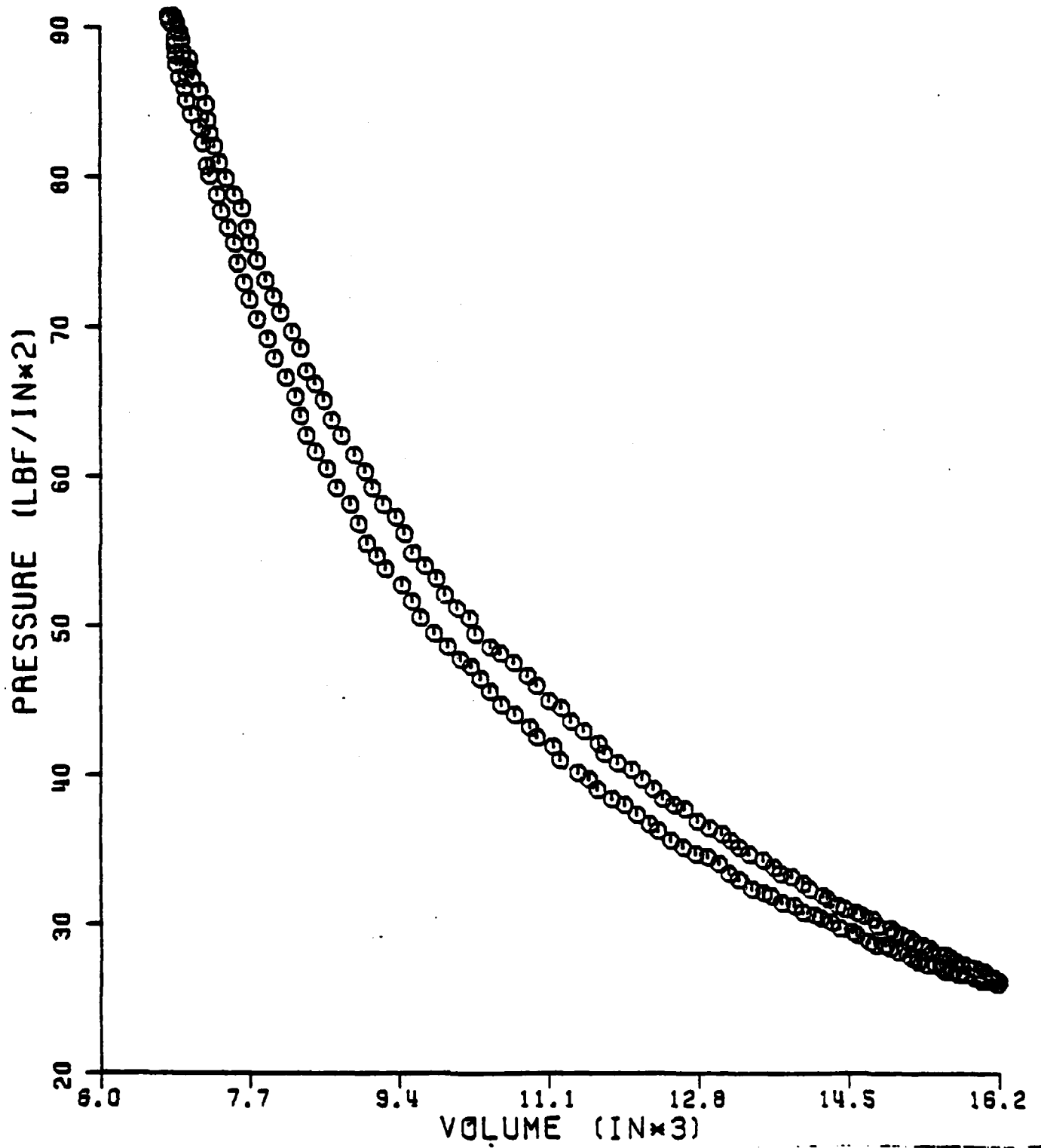
106	86.560	6.91	682.84	-0.10327	1.9107	0.7336	1.2201	-0.13543
107	87.428	6.88	686.58	-0.10002	1.9298	0.7303	1.2268	-0.13117
108	88.080	6.86	690.13	-0.09520	1.9442	0.7286	1.2331	-0.12485
109	88.731	6.85	693.66	-0.09046	1.9586	0.7269	1.2394	-0.11863
110	89.165	6.85	697.05	-0.08400	1.9682	0.7269	1.2455	-0.11016
111	90.034	6.83	702.24	-0.07620	1.9873	0.7253	1.2547	-0.09993
112	90.251	6.80	700.73	-0.06309	1.9921	0.7220	1.2520	-0.10896
113	90.468	6.79	700.81	-0.08496	1.9969	0.7203	1.2522	-0.11142
114	90.685	6.77	700.87	-0.08686	2.0017	0.7187	1.2523	-0.11391
115	90.685	6.80	704.10	-0.07674	2.0017	0.7220	1.2581	-0.10064
116	90.468	6.80	702.41	-0.07991	1.9969	0.7220	1.2550	-0.10479
117	90.685	6.83	707.32	-0.06666	2.0017	0.7253	1.2638	-0.08743
118	90.468	6.85	707.24	-0.06481	1.9969	0.7269	1.2637	-0.08500
119	90.251	6.86	707.14	-0.06299	1.9921	0.7286	1.2635	-0.08260
120	89.817	6.88	705.34	-0.06437	1.9825	0.7303	1.2603	-0.08442
121	89.599	6.91	706.82	-0.05761	1.9778	0.7336	1.2629	-0.07555
122	89.165	6.93	704.98	-0.05908	1.9682	0.7352	1.2596	-0.07747
123	88.297	6.94	699.68	-0.06707	1.9490	0.7369	1.2502	-0.08796
124	87.863	7.02	704.05	-0.04900	1.9394	0.7451	1.2580	-0.06426
125	87.211	7.00	697.28	-0.06374	1.9250	0.7435	1.2459	-0.08359
126	86.560	7.05	696.69	-0.05900	1.9107	0.7484	1.2448	-0.07738
127	85.692	7.13	697.32	-0.04813	1.8723	0.7567	1.2468	-0.06311
128	84.823	7.21	697.79	-0.03765	1.8484	0.7666	1.2335	-0.04938
129	83.738	7.22	690.35	-0.04993	1.8484	0.7666	1.2335	-0.06548
130	82.869	7.25	686.13	-0.05423	1.8292	0.7699	1.2260	-0.07112
131	82.001	7.30	683.32	-0.05402	1.8100	0.7749	1.2209	-0.07084
132	80.915	7.36	680.02	-0.05291	1.7861	0.7815	1.2150	-0.06939
133	79.830	7.44	678.00	-0.04758	1.7621	0.7898	1.2114	-0.06240
134	78.744	7.53	677.18	-0.03818	1.7381	0.7997	1.2100	-0.05007
135	77.876	7.61	676.63	-0.03018	1.7190	0.8079	1.2090	-0.03958
136	76.573	7.67	670.76	-0.03453	1.6902	0.8146	1.1985	-0.04528
137	75.488	7.70	663.93	-0.04448	1.6663	0.8179	1.1863	-0.05834
138	74.402	7.78	661.00	-0.04148	1.6423	0.8261	1.1810	-0.05440
139	73.100	7.89	658.52	-0.03418	1.6136	0.8377	1.1766	-0.04482
140	72.014	7.97	655.14	-0.03232	1.5896	0.8460	1.1706	-0.04239
141	70.929	8.05	651.57	-0.03098	1.5656	0.8542	1.1642	-0.04063
142	69.626	8.19	650.74	-0.01743	1.5369	0.8691	1.1627	-0.02286
143	68.541	8.28	647.91	-0.01320	1.5129	0.8790	1.1577	-0.01731
144	67.021	8.34	638.31	-0.02634	1.4794	0.8856	1.1405	-0.03455
145	66.153	8.44	637.09	-0.01904	1.4602	0.8955	1.1383	-0.02497
146	65.067	8.55	634.73	-0.01263	1.4362	0.9071	1.1341	-0.01656
147	63.765	8.64	628.83	-0.01541	1.4075	0.9170	1.1236	-0.02020
148	62.679	8.75	625.92	-0.01047	1.3835	0.9286	1.1184	-0.01374
149	61.376	8.89	622.73	-0.00321	1.3548	0.9435	1.1127	-0.00422
150	60.291	9.01	620.29	-0.00387	1.3308	0.9567	1.1083	-0.00507
151	59.205	9.09	614.39	-0.00120	1.3069	0.9650	1.0978	-0.00158
152	58.120	9.21	611.39	0.00433	1.2829	0.9782	1.0924	0.00567
153	57.252	9.35	611.41	0.01769	1.2637	0.9931	1.0924	0.02320

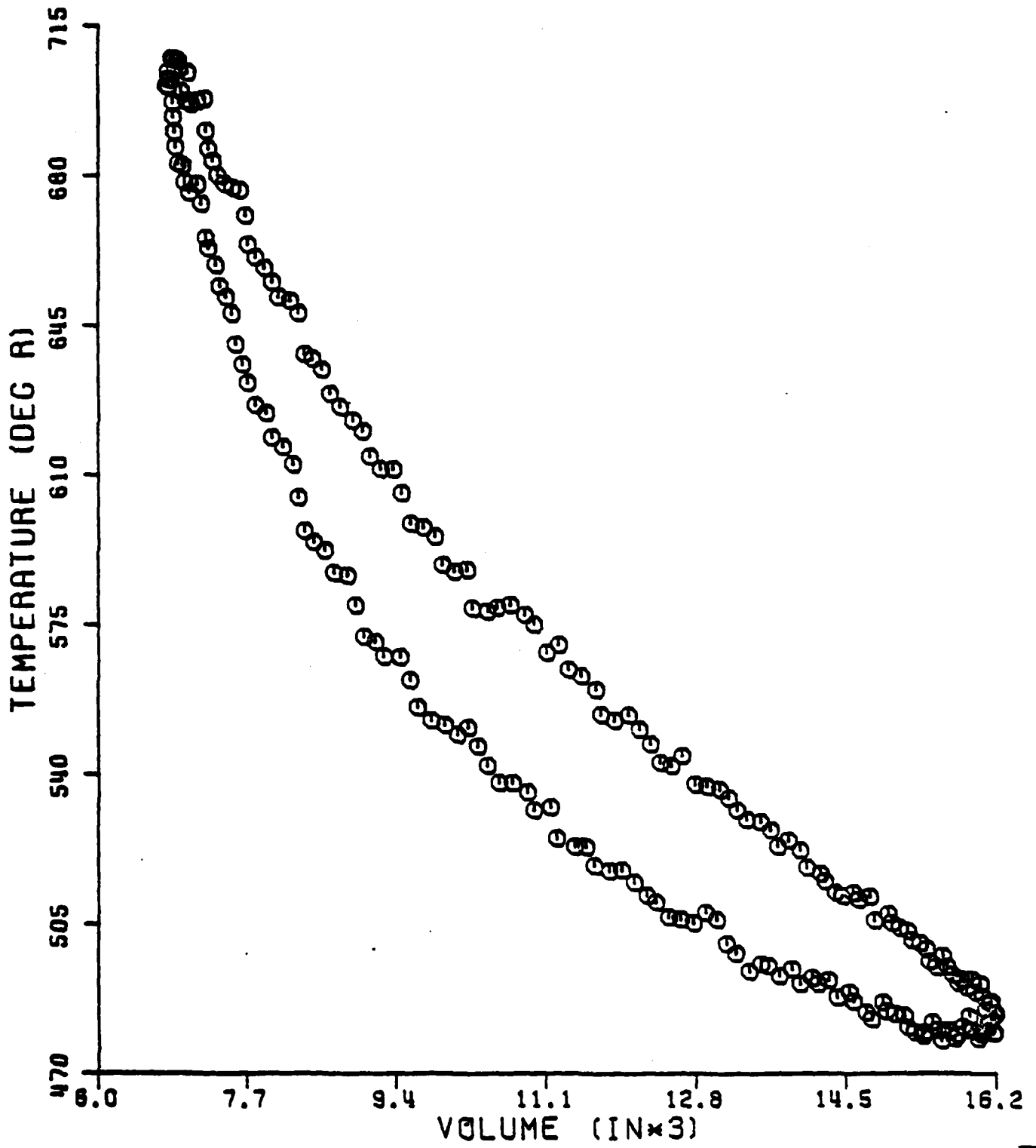
154	56.166	9.45	605.81	0.01427	1.2398	1.0030	1.0824	0.01872
155	54.663	9.56	598.58	0.00852	1.2110	1.0146	1.0695	0.01117
156	53.995	9.70	597.75	0.01951	1.1918	1.0294	1.0680	0.02559
157	53.127	9.82	595.69	0.02620	1.1727	1.0427	1.0644	0.03436
158	52.041	9.92	589.07	0.01976	1.1487	1.0526	1.0525	0.02592
159	51.173	10.06	587.42	0.02845	1.1296	1.0674	1.0496	0.03731
160	50.521	10.20	588.03	0.04202	1.1152	1.0823	1.0507	0.05510
161	49.436	10.26	578.91	0.02671	1.0912	1.0889	1.0344	0.03503
162	48.568	10.43	578.24	0.03978	1.0720	1.1071	1.0332	0.05217
163	48.133	10.54	579.06	0.05082	1.0625	1.1187	1.0346	0.06665
164	47.482	10.69	579.66	0.06514	1.0481	1.1352	1.0357	0.08542
165	46.614	10.85	577.35	0.07259	1.0289	1.1517	1.0316	0.09520
166	45.962	10.96	575.00	0.07602	1.0145	1.1633	1.0274	0.09969
167	44.877	11.10	568.60	0.07241	0.9906	1.1782	1.0160	0.09497
168	44.443	11.24	570.21	0.08722	0.9810	1.1931	1.0188	0.11438
169	43.574	11.35	564.49	0.08239	0.9618	1.2046	1.0086	0.10805
170	42.923	11.49	562.91	0.08953	0.9475	1.2195	1.0058	0.11741
171	42.055	11.66	559.75	0.09512	0.9283	1.2377	1.0001	0.12475
172	41.403	11.72	554.02	0.08622	0.9139	1.2443	0.9899	0.11307
173	40.752	11.88	552.55	0.09434	0.8995	1.2608	0.9873	0.12372
174	40.318	12.03	553.83	0.10889	0.8899	1.2774	0.9896	0.14280
175	39.666	12.16	550.53	0.11005	0.8756	1.2906	0.9837	0.14432
176	39.015	12.28	547.03	0.11062	0.8612	1.3038	0.9774	0.14142
177	38.364	12.39	542.68	0.10783	0.8468	1.3154	0.9696	0.14508
178	37.930	12.52	541.93	0.11483	0.8372	1.3286	0.9683	0.15059
179	37.713	12.64	544.19	0.12907	0.8324	1.3418	0.9723	0.16927
180	36.844	12.78	537.55	0.12256	0.8133	1.3567	0.9605	0.16073
181	36.410	12.92	537.04	0.13092	0.8037	1.3716	0.9596	0.17170
182	35.976	13.06	536.39	0.13884	0.7941	1.3865	0.9584	0.18208
183	35.542	13.17	534.34	0.14110	0.7845	1.3980	0.9547	0.18504
184	35.107	13.26	531.56	0.14043	0.7749	1.4079	0.9498	0.18416
185	34.673	13.37	529.30	0.14201	0.7654	1.4195	0.9457	0.18623
186	34.239	13.53	528.76	0.15086	0.7558	1.4360	0.9448	0.19785
187	33.805	13.65	526.86	0.15419	0.7462	1.4493	0.9414	0.20221
188	33.371	13.73	523.06	0.14962	0.7366	1.4575	0.9346	0.19622
189	33.153	13.85	524.37	0.16090	0.7318	1.4707	0.9369	0.21101
190	32.719	13.98	522.15	0.16320	0.7222	1.4840	0.9330	0.21402
191	32.285	14.06	518.09	0.15777	0.7126	1.4922	0.9257	0.20690
192	31.851	14.21	516.79	0.16414	0.7031	1.5088	0.9234	0.21526
193	31.634	14.26	514.95	0.16233	0.6983	1.5137	0.9201	0.21289
194	31.200	14.38	512.32	0.16322	0.6887	1.5269	0.9154	0.21406
195	30.982	14.46	511.51	0.16589	0.6839	1.5352	0.9139	0.21755
196	30.765	14.59	512.30	0.17550	0.6791	1.5484	0.9154	0.23015
197	30.548	14.65	510.86	0.17552	0.6743	1.5550	0.9128	0.23019
198	30.331	14.77	511.54	0.18476	0.6695	1.5683	0.9140	0.24230
199	29.897	14.82	505.81	0.17264	0.6599	1.5732	0.9038	0.22641
200	29.680	14.98	507.41	0.18605	0.6551	1.5898	0.9066	0.24399
201	29.463	15.02	505.27	0.18320	0.6503	1.5947	0.9028	0.24025

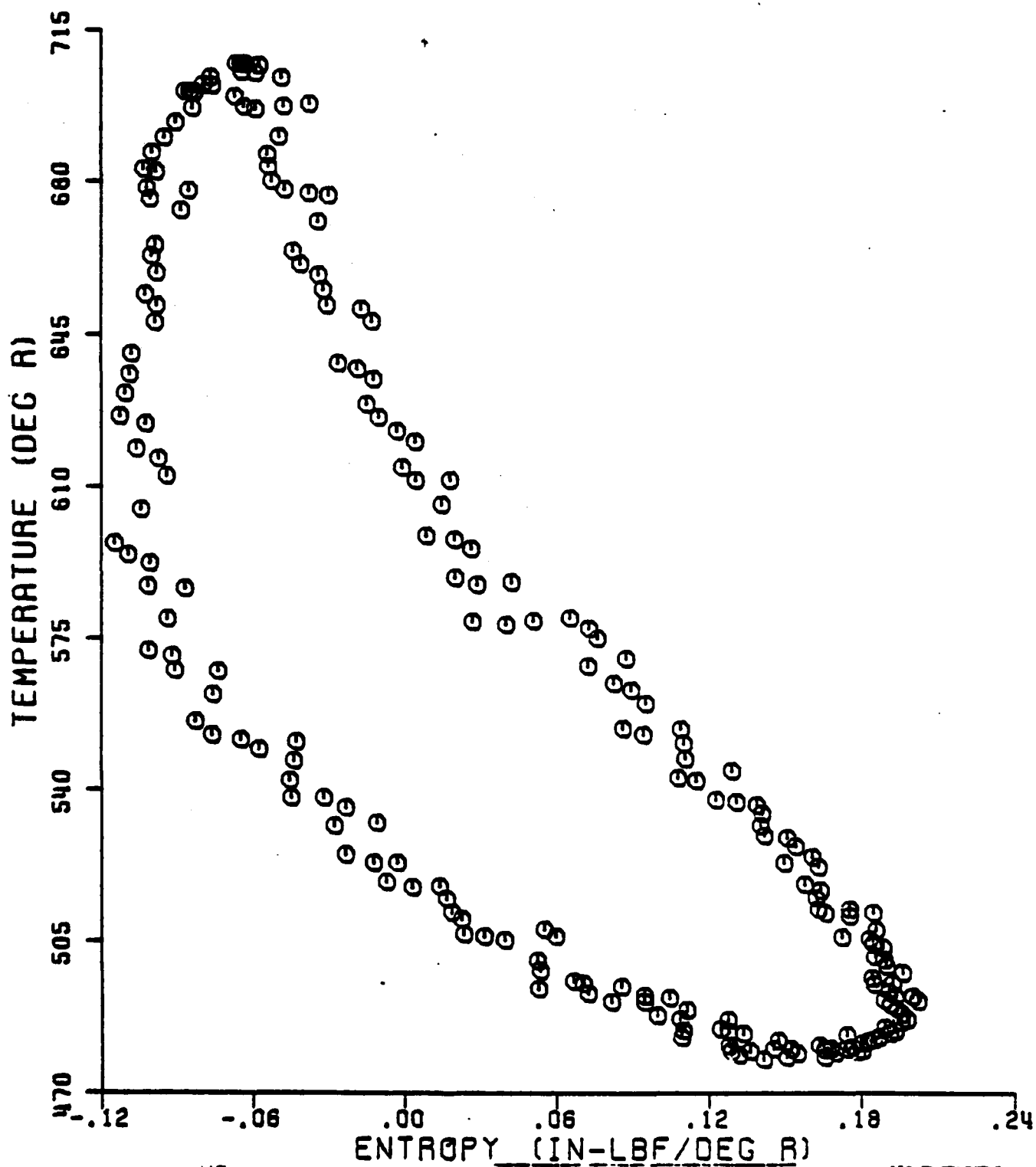
202	29.246	15.10	504.15	0.18481	0.6455	1.6030	0.9008	0.24237
203	29.029	15.19	503.50	0.18855	0.6408	1.6129	0.8996	0.24728
204	28.811	15.24	501.27	0.18539	0.6360	1.6179	0.8957	0.24313
205	28.594	15.33	500.54	0.18886	0.6312	1.6278	0.8944	0.24768
206	28.377	15.41	499.27	0.18994	0.6264	1.6360	0.8921	0.24910
207	28.160	15.44	496.45	0.18423	0.6216	1.6393	0.8870	0.24161
208	27.943	15.52	495.10	0.18508	0.6168	1.6476	0.8846	0.24272
209	27.943	15.60	497.59	0.19611	0.6168	1.6559	0.8891	0.25719
210	27.726	15.65	495.20	0.19239	0.6120	1.6608	0.8848	0.25231
211	27.509	15.71	493.28	0.19075	0.6072	1.6674	0.8814	0.25016
212	27.292	15.77	491.33	0.18899	0.6024	1.6741	0.8779	0.24785
213	27.292	15.80	492.30	0.19334	0.6024	1.6774	0.8796	0.25356
214	27.075	15.86	490.30	0.19145	0.5976	1.6840	0.8761	0.25108
215	27.075	15.93	492.23	0.20009	0.5976	1.6906	0.8795	0.26241
216	27.075	15.93	492.23	0.20009	0.5976	1.6906	0.8795	0.26241
217	26.858	15.96	489.24	0.19375	0.5928	1.6939	0.8742	0.25409
218	26.858	16.02	491.15	0.20234	0.5928	1.7005	0.8776	0.26535
219	26.640	16.05	488.12	0.19588	0.5880	1.7038	0.8722	0.25689
220	26.206	16.07	480.63	0.17628	0.5785	1.7055	0.8588	0.23118
221	26.423	16.08	485.09	0.18933	0.5833	1.7071	0.8667	0.24829
222	26.423	16.13	486.49	0.19572	0.5833	1.7121	0.8693	0.25668
223	26.206	16.14	482.96	0.18694	0.5785	1.7137	0.8629	0.24516
224	26.423	16.14	486.96	0.19785	0.5833	1.7137	0.8701	0.25947
225	26.206	16.14	482.96	0.18694	0.5785	1.7137	0.8629	0.24516

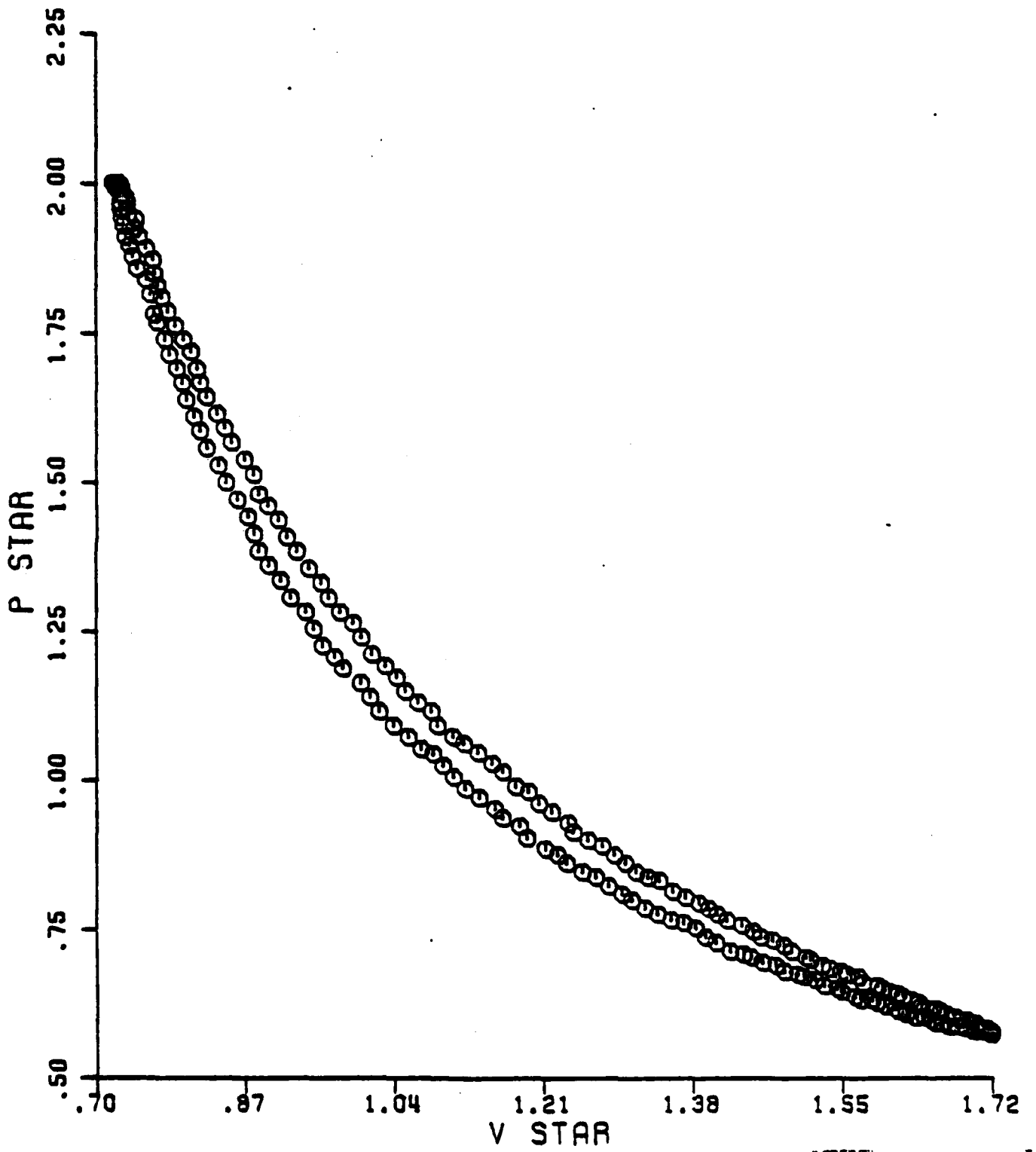
APPENDIX D

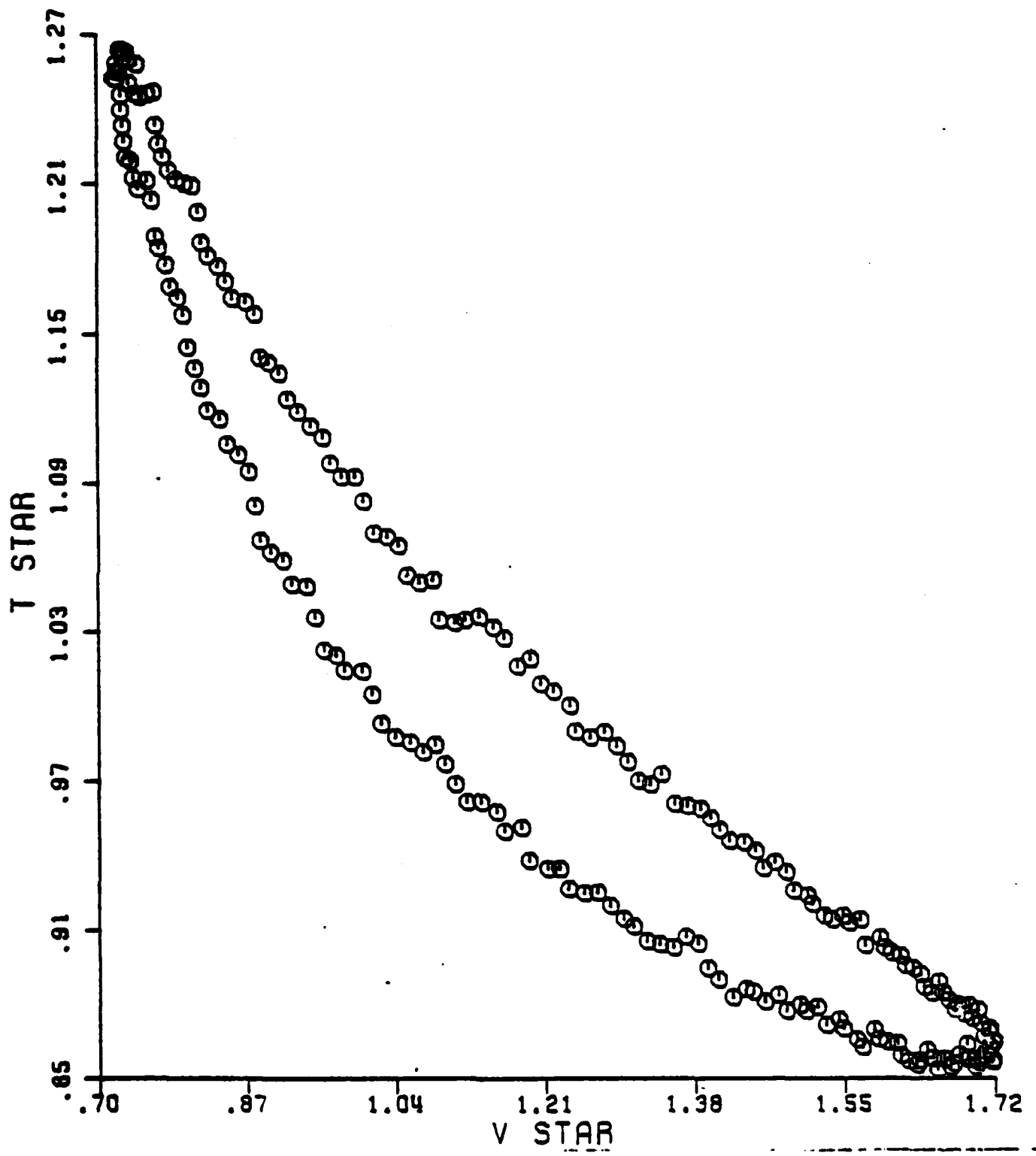
CYCLE PROGRAM PLOTS OUTPUT

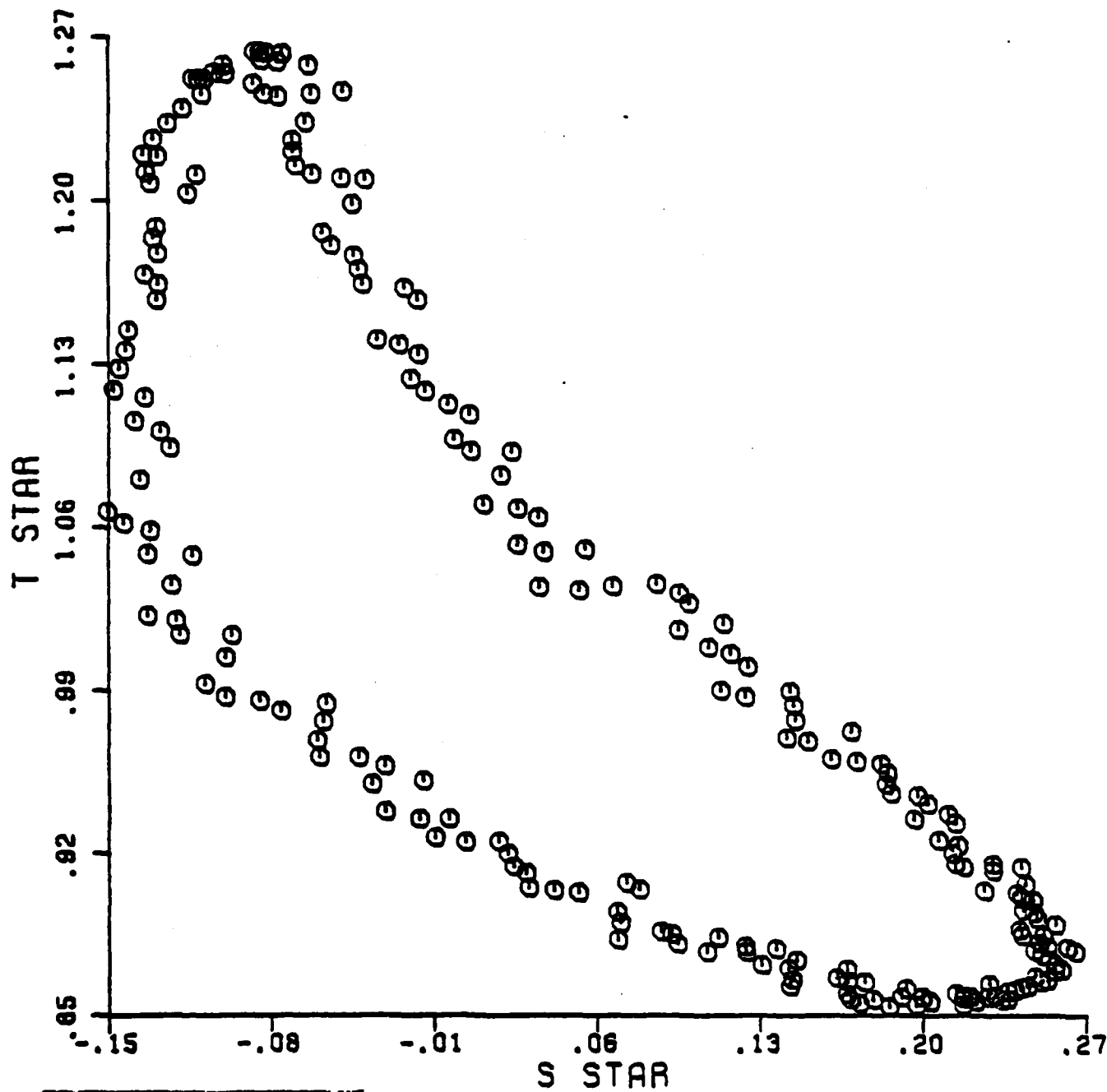












83

END

FILMED

11-83

DTIC